HHS Public Access

Author manuscript

Immunity. Author manuscript; available in PMC 2024 August 08.

Published in final edited form as:

Immunity. 2023 August 08; 56(8): 1862–1875.e9. doi:10.1016/j.immuni.2023.06.022.

The gut protist *Tritrichomonas arnold* restrains virus-mediated loss of oral tolerance by modulating dietary antigen-presenting dendritic cells

Luzmariel Medina Sanchez[1,2,16], **Magdalena Siller**[1,16], **Yanlin Zeng**[1,3,16], **Pamela H. Brigleb**[2,4,5], **Kishan A. Sangani**[6,7], **Ariadna S. Soto**[1], **Clarisse Engl**[1], **Colin R. Laughlin**[1], **Mohit Rana**[1], **Lauren Van Der Kraak**[1], **Surya P. Pandey**[1], **Mackenzie J. Bender**[1], **Britney Fitzgerald**[1], **Lee Hedden**[1], **Kay Fiske**[5,8], **Gwen M. Taylor**[5,8], **Austin P. Wright**[9], **Isha D. Mehta**[1], **Syed A Rahman**[1,10], **Heather J. Galipeau**[11], **Steven J. Mullett**[12,13], **Stacy L. Gelhaus**[12,13], **Simon C. Watkins**[14], **Premysl Bercik**[11], **Timothy J. Nice**[9], **Bana Jabri**[6,7], **Marlies Meisel**[1,15], **Jishnu Das**[1,10], **Terence S. Dermody**[4,5,8], **Elena F. Verdú**[11], **Reinhard Hinterleitner**[1,5,15,17,*]

[1]Department of Immunology, University of Pittsburgh School of Medicine, Pittsburgh, PA, USA

[2]Graduate Program in Microbiology and Immunology, University of Pittsburgh School of Medicine, Pittsburgh, PA, USA

[3]School of Medicine, Tsinghua University, Beijing, China

[4]Department of Microbiology and Molecular Genetics, University of Pittsburgh School of Medicine, Pittsburgh, PA, USA

[5]Institute of Infection, Inflammation, and Immunity, UPMC Children's Hospital of Pittsburgh, Pittsburgh, PA, USA

[6]Department of Medicine, University of Chicago, Chicago, IL, USA

[7]Committee on Immunology, University of Chicago, Chicago, IL, USA

[8]Department of Pediatrics, University of Pittsburgh School of Medicine, Pittsburgh, PA, USA

[9]Department of Molecular Microbiology and Immunology, Oregon Health & Science University, Portland, OR, USA

[*]Correspondence: reinhard@pitt.edu (R.H).

AUTHOR CONTRIBUTIONS

Conceptualization: R.H. Methodology: L.M.S., M.S., Y.Z., P.H.B., K.A.S., A.S.S., C.L., M.R., L.V.D.K., S.P.P., A.P.W., I.D.M., S.J.M. Investigation: L.M.S., M.S., Y.Z., P.H.B., K.A.S., A.S.S., C.E., C.L., M.R., L.V.D.K., S.P.P., M.J.B., B.F., L.H., K.F., G.M.T., A.P.W., I.D.M., S.A.R., H.J.G., S.J.M., M.M., R.H. Visualization: K.A.S., C.L., M.R., R.H. Funding acquisition: S.L.G., M.M., B.J., T.S.D., E.F.V., R.H. Project administration: R.H. Supervision: S.L.G., S.C.W., P.B., T.J.N., M.M., B.J., J.D., T.S.D., E.F.V., R.H. Writing original draft: R.H. Writing – review and editing: L.M.S., M.S., Y.Z., M.M., B.J., T.S.D., E.F.V., R.H.

DECLERATION OF INTERESTS

E.F.V is Member of the Biocodex International and National (Canada) Scientific Review Boards, Member of the Center for Gut Microbiome Research and Education Scientific Advisory Board of the AGA, Secretary of the International Society of the Study of Celiac Disease, and holds grants from Kallyope and Codexis, unrelated to this study. H.J.G holds a grant from Codexis, unrelated to this study.

[10]Center for Systems Immunology, Departments of Immunology and Computational & Systems Biology, University of Pittsburgh School of Medicine, Pittsburgh, PA, USA

[11]Farncombe Family Digestive Health Research Institute, Department of Medicine, McMaster University, Hamilton, Ontario, Canada

[12]Department of Pharmacology and Chemical Biology, University of Pittsburgh School of Medicine, Pittsburgh, PA, USA

[13]Health Sciences Mass Spectrometry Core, University of Pittsburgh, Pittsburgh, PA, USA

[14]Department of Cell Biology, University of Pittsburgh School of Medicine, Pittsburgh, PA, USA

[15]Cancer Immunology and Immunotherapy Program, UPMC Hillman Cancer Center; Pittsburgh, PA, USA

[16]These authors contributed equally

[17]Lead contact

SUMMARY

Loss of oral tolerance (LOT) to gluten, driven by dendritic cell (DC) priming of gluten-specific T helper 1 (Th1) cell immune responses, is a hallmark of celiac disease (CeD) and can be triggered by enteric viral infections. Whether certain commensals can moderate virus-mediated LOT remains elusive. Here, using a mouse model of virus-mediated LOT, we discovered that the gut colonizing protist *Tritrichomonas (T.) arnold* promotes oral tolerance and protects against reovirus- and murine norovirus-mediated LOT, independent of the microbiota. Protection was not attributable to antiviral host responses or *T. arnold*-mediated innate type-2 immunity. Mechanistically, *T. arnold* directly restrained the proinflammatory program in dietary antigen-presenting DCs, subsequently limiting Th1 and promoting regulatory T cell responses. Finally, analysis of fecal microbiomes showed that *T. arnold*-related *Parabasalid* strains are underrepresented in human CeD patients. Altogether, these findings will motivate further exploration of oral-tolerance-promoting protists in CeD and other immune-mediated food sensitivities.

Graphical Abstract

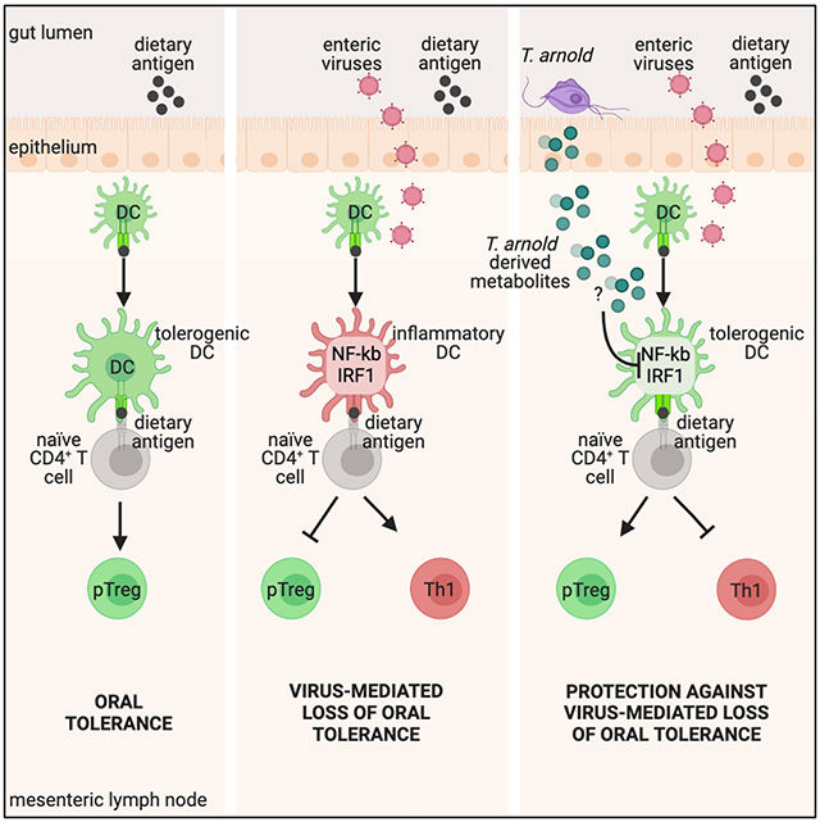

eTOC

Enteric viruses can trigger loss of oral tolerance to dietary gluten resulting in the development of Celiac disease. Medina Sanchez et al. discovered *Tritrichomonas arnold*, a previously undescribed murine gut commensal protist capable of preventing virus-mediated loss of oral tolerance by directly restraining proinflammatory dendritic cell function.

INTRODUCTION

Celiac disease (CeD) is an immune disorder in which genetically susceptible individuals expressing the human leukocyte antigen (HLA) DQ2 or DQ8 molecules display an inflammatory T helper 1 (Th1) cell immune response against dietary gluten present in wheat, barley, and rye that results in loss of oral tolerance to gluten (LOT) [1-3]. Elimination of gluten from the diet is the current and only standard of care. With its high prevalence among the general population (1-2%), challenges of maintaining a gluten free diet (GFD), poor efficacy of GFD in 40-60% of CeD patients, and associated risks for other autoimmune diseases and cancer, CeD is a significant cause of disease and disability [4,5]. The HLA-DQ2- or DQ8-restricted Th1 cell response against gluten initiates CeD pathogenesis, characterized by cytotoxic intraepithelial $CD8^+$ lymphocyte-mediated tissue destruction resulting in villous atrophy [6,7]. Dendritic cells (DCs) play a central role in maintaining tolerance to dietary antigens such as gluten. During homeostasis, tolerogenic DCs sample dietary antigens from the intestinal lumen and migrate to the mesenteric lymph nodes (mLN), the

inductive site of oral tolerance. DCs promote dietary antigen-specific regulatory T (Treg) cell responses, and consequently sustain oral tolerance [8,9]. In CeD, the suppression of gluten-specific immunity is impaired, characterized by proinflammatory DC responses that subsequently lead to dampened Treg and heightened proinflammatory Th1 cell responses against gluten [1-3,10]. LOT to gluten is central to CeD pathogenesis and precedes the development of villous atrophy [6].

Even though approximately 30% of the human population carry HLA DQ2 or DQ8, only 1% develop CeD [1], suggesting that additional factors contribute to CeD pathogenesis. Viruses have been implicated as potential environmental triggers in CeD pathogenesis [11-14]. Concordantly, we showed previously that reovirus, a largely avirulent pathogen that elicits protective immunity, can nonetheless promote LOT by suppressing Treg cell conversion and promoting inflammatory Th1 cell responses to dietary antigen. Mechanistically, the human reovirus isolate, type 1 Lang (T1L) mediates LOT by endowing dietary antigen presenting DCs with proinflammatory properties in the mesenteric lymph nodes (mLN) [15]. Using both reovirus and murine norovirus strains, we have shown that the capacity of a virus to disrupt tolerance to oral antigens is not determined by its viral family, but rather by its potential to trigger IRF1-dependent inflammatory pathways in the mLN [15,16]. Gut microbes have emerged as important modulators of mucosal immunity during homeostasis and in intestinal diseases, such as CeD [17-19]. The mammalian gut microbiome encompasses bacteria, archaea, viruses, fungi, and protists; all having a profound impact on gut immunity in health and disease. Protists are unicellular organisms that commonly inhabit mammalian intestines [20]. The majority of known and well-studied intestinal protists are pathogenic to humans [21,22] and other mammals [23]. The murine gut commensal protist *Tritrichomonas* sp. (class *Parabasalia*) can initiate strain- and location-dependent mucosal immune responses [24-28]. However, whether and how gut commensal protists impact mucosal immunity in CeD and thereby affect its etiopathogenesis remains enigmatic.

By using our previously defined reovirus-mediated LOT CeD model [15], here we showed that the gut protist *Tritrichomonas arnold* (*T. arnold*), which belongs to the class *Parabasalia*, promoted oral tolerance, and prevented virus-mediated LOT. Mechanistically, we showed that *T. arnold* modulates dietary antigen-presenting DCs to promote Treg cells and to restrain the virus-induced proinflammatory IRF1/NF-κB program, thereby limiting Th1 cell responses. *T. arnold*-mediated protection from virus-induced LOT was not specific to T1L but was also observed with murine norovirus strain CW3. Highlighting the translational relevance of our findings, analysis of stool samples of a cohort of CeD patients and healthy controls revealed that *Parabasalia* were underrepresented in CeD patients relative to healthy controls.

RESULTS

Suppression of T1L-induced LOT is associated with the presence of *Tritrichomonas* in in-housed mice.

In the course of our studies on reovirus T1L-mediated inflammatory responses to dietary antigen [15], we reproduced our findings using C57BL/6 mice commercially acquired from Jackson Laboratories (JAX). However, we did not observe T1L-mediated inflammatory

responses to dietary antigen in aged- and sex-matched C57BL/6 mice bred in our vivarium ("in-housed" mice originally acquired from JAX) using an oral tolerance assay (Figure 1A-C and Figure S1A-D). T1L-mediated $CD4^+$ Th1 cell immune responses specific for dietary antigen, characterized by elevated expression of interferon-γ (IFNγ) and T-box transcription factor 21 (Tbx21 encoding Tbet), were absent in in-housed mice when compared with JAX mice (Figure 1A-C and Figure S1B-D). Untreated and T1L-infected in-housed mice displayed an expansion of Treg cells compared with untreated and T1L-infected JAX mice, respectively (Figure 1A-C and Figure. S1B-D), suggesting that environmental factors present in in-housed but not JAX mice mediate protection against T1L-mediated LOT. T1L infection promoted host $Tbet^+$ $CD4^+$ T cell responses that were comparable between in-housed mice and JAX mice and concordant with our previous findings ((Figure S1E-G) and [15]), indicating that host Th1 cell responses to T1L infection are uncoupled from dietary-antigen-specific Th1 cell responses in in-housed mice. Dietary antigen uptake takes place in the small intestine [29,30]. Histological examination revealed an enlarged small intestine and an expansion of tuft and goblet cells in in-housed mice relative to JAX mice, independent of T1L infection (Figure 1D-F). These findings suggest an elevated type-2 immune response, which is usually observed in mice infected with helminths [31,32] or colonized with the gut commensal protist *Tritrichomonas* [24]. As helminth infections are unlikely, based on our specific-pathogen free (SPF) mouse facility status, we examined animals for *Tritrichomonas* in cecal contents. This analysis revealed the presence of *Tritrichomonas* in in-housed mice but not mice acquired from JAX (Figure 1G). Internal transcribed spacer (ITS) sequencing identified this protist as an uncharacterized *Tritrichomonas* sp. isolate with the accession number MF375342 and with 86%, 84%, and 85% homology to the ITS of *Tritrichomonas muris, Tritrichomonas musculis*, and *Tritrichomonas rainier*, respectively ((Figure S2A-B) and [24-26]). Although the precise taxonomic relationship of these tritrichomonads remains to be determined, for clarity we hereafter refer to the University of Pittsburgh isolate as *T. arnold*. Collectively, our findings demonstrate that the suppression of T1L-induced LOT is associated with the presence of *T. arnold* in the intestines of in-housed mice.

T. arnold promotes dietary antigen-specific Treg cell responses.

T. arnold colonization was observed along the small intestine, cecum, and colon to similar levels in naturally colonized in-housed mice and JAX WT mice orally gavaged with *T. arnold* (Figure 2A). Furthermore, dietary ovalbumin (OVA) failed to affect the ability of *T. arnold* to colonize the intestinal tract (Figure S2C). Next, we wanted to better understand how *T. arnold* colonization affects mucosal $CD4^+$ T cell responses to dietary OVA during homeostasis, in the absence of T1L infection (Figure S2D). We found that *T. arnold* colonization of JAX WT mice promoted an enhancement of dietary-antigen-specific Treg cells relative to controls (Figure 2B-D). Although *T. arnold* induced type-2 responses in the enteric mucosa (Figure 1E-F), we neither observed *T. arnold*-induced Th2 cell responses against dietary antigen nor *T. arnold*-induced Th2 cell responses in the polyclonal T cell pool in the mLN (Figure 2E and Figure S2E). In addition, *T. arnold* colonization failed to promote Th1 and Th17 cell differentiation against dietary antigen (Figure 2B-D and Figure 2F). Altogether, these findings suggest that *T. arnold* selectively drives dietary-antigen-specific Treg cell differentiation.

T. arnold protects against T1L-mediated LOT without impacting antiviral immunity and independent of the microbiota.

To test the sufficiency of *T. arnold* in protecting against T1L-mediated inflammatory responses to dietary antigen, we orally inoculated 6-week-old JAX WT mice with *T. arnold*. Twelve days post *T. arnold* colonization, we conducted an oral tolerance assay (Figure S3A). T1L infection failed to impact on the colonization efficiency of *T. arnold* (Figure S3B). Confirming previous observations [15], T1L blocked Treg cell responses and promoted Th1 cell responses specific for dietary antigens in the absence of T. arnold (Figure 3A-C). *T. arnold* efficiently counteracted both T1L-mediated Treg cell suppression and Th1 cell responses against dietary antigen (Figure 3A-C). *T. arnold* restored T1L-mediated Treg cell suppression to levels comparable to that of non-T1L infected *T. arnold* colonized mice (Figure S3C-D). *T. arnold* did not affect viral replication, anti-reovirus antibody titers, and host type-1 interferon responses (Figure 3D-F; Table S1), suggesting that *T. arnold*-mediated protection against T1L-induced LOT is not attributable to differences in antiviral host responses. To assess whether protection against T1L-mediated LOT requires active *T. arnold* colonization we put mice colonized with *T. arnold* (Figure 3G) on a cellulose-rich diet in the absence of water-soluble fibers. This diet regimen successfully depletes *Tritrichomonas* from the intestine [28]. We observed a 5-log fold reduction in relative abundance, suggesting that *T. arnold* was successfully depleted (Figure 3G). In contrast to our previous results (Figure 3A-C), mice cleared of *T. arnold* prior to an oral tolerance assay failed to protect against T1L-mediated LOT (Figure 3H). These findings indicate that active *T. arnold* colonization is sufficient and required to suppress virus-mediated LOT.

We next sought to determine how *T. arnold* confers the protective effect against T1L-mediated LOT. One possibility is that *T. arnold* influences oral tolerance indirectly by modulation of the microbiota. The short chain fatty acid (SCFA) butyrate produced by specific bacteria promotes tolerogenic immune responses and Treg cell differentiation [33]. We confirmed that *T. arnold*, similar to other *Tritrichomonas spp.*, is unable to produce butyrate [25] and (Figure S3E). Furthermore, *T. arnold* colonization did not alter butyrate concentrations within the cecum, indicating that *T. arnold*-mediated protection against virus-induced LOT is not due to increased microbial butyrate levels (Figure S3F). To directly test whether *T. arnold* requires the microbiota to protect against T1L-induced LOT, we conducted T cell conversion assays using germ-free WT mice monocolonized with *T. arnold*. We found that *T. arnold* protected from T1L-mediated LOT independent of a pre-established microbiome (Figure 3I-J).

Succinate and IL-25 are not sufficient to protect against T1L-mediated LOT and IL-18 is dispensable for *T. arnold*-mediated protection against T1L-mediated LOT.

Similar to studies using other *Tritrichomonas* spp. [24,25], *T. arnold* colonization of JAX mice for 2 weeks resulted in elevated type-2 immunity in the small intestine, characterized by tuft and goblet cell hyperplasia (Figure S4A-B). Typically, *Tritrichomonas* spp. promote type-2 immunity by releasing succinate, a carboxylic acid and fermentation product from the ingestion of complex polysaccharides [25,28] and (Figure S4C). Succinate is sensed by succinate-receptor-expressing tuft cells and is sufficient to promote IL-25-mediated tuft and goblet cell expansion and group 2 innate lymphoid cell (ILC2) activation [25,28,34]. As

observed previously [25,28,34], succinate supplementation in drinking water was sufficient to induce type-2 immune responses in the small intestine similar to *T. arnold* colonization in *Tritrichomonas*-free mice (Figures S4A-B and S4D-E). Next, we tested whether succinate supplementation in drinking water is sufficient to promote oral tolerance and protect against T1L-mediated LOT. Mice were administered succinate in drinking water for 12 days prior to an OT-II conversion assay (Figure S4F). In contrast to *T. arnold*, succinate alone was neither sufficient to promote Treg cell responses to dietary antigen nor capable of protecting against T1L-mediated LOT (Figure 4A-B). Succinate failed to influence viral replication and host Th1/Treg cell responses (Figure 4C-E). These data indicate that *T. arnold*-mediated oral tolerance is independent of the capacity of the protist to release succinate. Goblet cells are implicated in dietary antigen uptake and oral tolerance [35,36]. Although we observed an expansion of goblet cells in *T. arnold*-colonized mice (Figure S4B), the fact that succinate supplementation induced similar levels of goblet cell expansion (Figure S4E) suggests that goblet cell expansion alone cannot explain the immunologic tolerance to dietary antigen induced by *T. arnold*. Similar to previous studies [24,37], daily IL-25 treatment (Figure S4G) led to a robust tuft cell expansion in the gut (Figure S4H) and expansion of ILC2 in the mLN (Figure 4F), a tissue site where oral tolerance is initiated. However, IL-25 induced type-2 immunity was neither sufficient to prevent T1L-mediated Th1 cell responses to dietary antigen nor to restore dietary antigen specific Treg cell responses (Figure 4G-H). IL-25 also failed to impact host Th1 and Treg cell responses in the mLN. (Figure 4I-J). Collectively, we show that *T. arnold* colonization promotes oral tolerance and prevents T1L-mediated LOT independent of succinate and IL-25 signaling.

T. musculis promotes IL-18 release by colonocytes, which confers protection against *Salmonella typhimurium* infection [26]. To determine whether IL-18 functions in the protective effects of *T. arnold* in reovirus-induced LOT, we conducted an OT-II conversion assay using IL-18 deficient mice. *T. arnold* protected against T1L-induced LOT to a comparable extent in IL-18 deficient mice and WT controls, suggesting that IL-18 is dispensable for the effects of *T. arnold* on dietary-antigen-specific immune responses (Figure S4I-J).

T. arnold restrains the T1L-induced proinflammatory program in dietary antigen-presenting DCs.

DCs orchestrate protective and tolerogenic T cell responses to reovirus infection and dietary antigen, respectively [8,9,38]. In Peyer's patches (PP), protective immunity to T1L is initiated by viral antigen processing $CD103^{-}$ $CD11b^{+}$ DCs [38]. In contrast, in mLN, tolerogenic $CD103^{+}$ DCs present dietary antigen and induce oral tolerance [29]. Dietary antigen-presenting $CD103^{+}$ $CD11b^{-}$ $CD8a^{+}$ conventional type 1 DCs (cDC1) have the highest tolerogenic potential [8,15,39] but also drive Th1 cell responses to enteric pathogens [9,15,40,41]. We previously showed that T1L infection induces an interferon regulated factor 1 (IRF1)-mediated proinflammatory program in cDC1, characterized by elevated interleukin 12 (IL-12) production, activation of the costimulatory molecule CD86, and increased *Il27* gene expression, that subsequently promotes LOT [15]. Based on our finding that *T. arnold* blocks T1L-mediated inflammatory responses to dietary antigen, we determined whether *T. arnold* prevents T1L-mediated inflammatory DC responses in PP and mLN, respectively.

As expected, flow cytometric analysis of DCs in PP and mLN revealed that T1L infection induces inflammatory DC activation as evidenced by IL-12 production and upregulation of CD86 at both sites (Figure 5A-F and Figure S5A-B). Strikingly, *T. arnold* colonization specifically suppressed T1L-mediated IL-12 production and CD86 and *Il27* expression in DCs, including cDC1 in mLN but not in the PP (Figure 5A-G and Figure S5A-B) suggesting that *T. arnold* protects against T1L-mediated LOT by suppressing inflammatory cDC1 responses specifically in the mLN. Furthermore, the observation that *T. arnold* failed to restrain T1L-mediated inflammatory responses in PP is consistent with our finding that *T. arnold* prevented T1L-mediated LOT without affecting the antiviral host immunity (Figure 3D-F). T1L-mediated IL-12 production and expression of CD86 in mLN cDC1 of *T. arnold* colonized mice remained elevated when compared to PBS and *T. arnold* control groups (Figure 5D-F), but the level of DC activation was insufficient to either prevent Treg or promote Th1 cell induction to dietary antigens (Figure 3A-C and Figure S3C-D). $CD103^+$ DCs in the small intestinal *lamina propria* take up dietary antigens and migrate to the mLN to present dietary antigen to $CD4^+$ T cells [8,39]. *T. arnold* colonization did not affect the overall composition of mLN DC subsets, efficiency of dietary OVA-antigen uptake by mLN DCs or OT-II T cell proliferation (Figure S5C-E), suggesting that *T. arnold* does not impact the presence of dietary antigen-presenting DCs at inductive sites of oral tolerance and their ability to present dietary antigen to OT-II T cells. To better understand how *T. arnold* colonization impacts the T1L-mediated proinflammatory response in dietary antigen-presenting cDC1, we examined the transcriptional profile of mLN-derived cDC1. We found increased expression of the transcription factor *Irf1* in cDC1 from T1L infected mice compared to PBS and *T. arnold* colonized mice (Figure 5H-I; Table S2), which is required for T1L- and CW3-mediated induction of the Th1-promoting cytokines IL-12 and IL-27 and LOT in these models [15,16]. *T. arnold* suppressed T1L-induced expression of *Irf1* in cDC1 (Figure 5I-J; Table S2). The transcription factors Nuclear factor κB (NF-κB) and IRF1 are important regulators of inflammatory immune responses in cDC1, and their involvement to promote Th1 cell responses has been previously shown by studying the gene expression profile of *Irf1*-deficient and *Ikbkb*-deficient intratumoral cDC1 [42]. Analysis of differentially expressed genes (DEGs) between T1L and T1L + *T. arnold* revealed a significant enrichment for the NF-κB pathway and in genes harboring transcription factor binding sites for Irf1, Irf8, and NF-κB (Figure S5F-G). We next assessed DEGs that were regulated in an IRF1 and/or NF-κB dependent manner [42] and had increased expression in the T1L group compared to the PBS group. Here we found that cDC1 from T1L infected mice had increased gene expression levels for activation markers, Th1 cell associated markers, and IFN-regulated genes such as *Cd40*, *Cd274* (PDL1), *Ccl5*, *Il27*, *Isg15*, and *Mx1* (Figure 5K). Comparison of cDC1 gene expression profiles showed that the presence of *T. arnold* restrained the induction of the majority of IRF1 and/or NF-κB regulated genes (Figure 5K). These findings suggest that the suppression of the T1L-induced transcription factors IRF1 and/or NF-κB in cDC1 by *T. arnold* is a possible mechanism of how *T. arnold* protects against T1L-induced LOT.

Given our observation that *T. arnold* promoted dietary antigen-specific Treg cells during homeostasis (Figure 2B-D) we examined the transcriptional profile of mLN-derived cDC1 to investigate whether *T. arnold* colonization promotes a tolerogenic program in cDC1 in

the absence of T1L infection. DEG analysis in mLN cDC1 between PBS and *T. arnold* did not reveal any differences in genes primarily involved in Treg cell differentiation such as TGFβ and retinoic acid (Figure S5H; Table S2). However, we identified two DEGs, *Cdk19* and *Clec7a* (Dectin1), with decreased expression in the *T. arnold* group compared to the PBS group that play a role in tolerogenic DC responses [43,44]. Cdk19 blockade will drive IL-10 production in DCs [43], while Dectin1 deficiency promotes tolerogenic DC responses and increased Treg cell differentiation [44]. We next assessed whether *T. arnold* directly acts on mLN DCs to promote tolerance at steady state. Thus, we performed *ex vivo* co-cultures of mLN derived DCs from *T. arnold* colonized mice with naïve $CD4^+$ OT-II T cells and OVA peptide in the presence of suboptimal TGFβ concentration. We found that the presence of *T. arnold in vivo* promoted increased OVA-specific Treg cell responses compared to PBS treated mice *ex vivo* (Figure S5I). Taken together these findings suggest that *T. arnold* colonization during homeostasis, in the absence of T1L infection, directly acts on DCs to promote dietary antigen specific Treg cell responses in the mLN.

Most important to our model, we next set out to interrogate whether *T. arnold*-mediated suppression of the T1L-induced inflammatory IRF1/NF-κB program of dietary antigen-specific DCs affects the ability of DCs to promote Th1 cell responses. To this end, we performed *ex vivo* co-cultures of mLN-derived DCs isolated 48 hours after T1L inoculation in the presence or absence of *T. arnold* colonization with naïve $CD4^+$ OT-II T cells and OVA peptide. We found that *T. arnold* directly acts on DCs *in vivo* to mediate suppression of T1L-induced inflammatory Th1 cell responses *ex vivo*. (Figure 5L-M). To test whether *T. arnold*-derived metabolites are sufficient to prevent T1L-induced Th1 cell responses, we pre-incubated mLN-derived DCs isolated 48 hours after T1L inoculation with *T. arnold*-derived cell culture supernatant. We found that *T. arnold* derived metabolites restrain Th1 cell differentiation, shown by a decrease in Tbet expression (Figure 5N), suggesting that *T. arnold* mediated protection against T1L-induced LOT may in part be driven by *T. arnold*-derived metabolites.

Comparable to T1L, CW3 mediates inflammatory responses to dietary antigen in an IRF1-dependent manner [15,16]. Given our findings that *T. arnold* suppressed a T1L-induced inflammatory IRF1/NF-κB program in dietary antigen-presenting cDC1s (Figure 5I-K and Figure S5F-G), we next addressed the question of whether *T. arnold* is sufficient to suppress CW3-induced LOT. Colonization with *T. arnold* indeed suppressed CW3-mediated Th1 cell responses to dietary antigen without affecting anti-viral host responses (Figures 5O and Figure S5J-K).

Collectively, our findings demonstrate that *T. arnold* protects against virus-induced LOT, using two different virus strains that have previously been shown to mediate LOT in an IRF1-dependent manner [15,16], suggesting that *T. arnold* confers protection by suppressing the virus-induced inflammatory IRF1/NF-κB program in dietary antigen-presenting cDC1.

Parabasalia protect against LOT to gluten and are underrepresented in CeD patients.

To determine the relevance of these findings to CeD, we analyzed the effect of *T. arnold* colonization on T1L-mediated LOT to gluten in transgenic mice expressing the CeD-predisposing HLA molecule DQ8 (DQ8tg mice) [15]. Whereas T1L induced LOT to

gluten in mice without *T. arnold* colonization, the presence of *T. arnold* prevented T1L-mediated LOT to gluten in DQ8tg mice, as assessed by the presence of anti-gliadin IgG2c antibodies and the development of a Th1 delayed-type hypersensitivity (DTH) reaction (Figure 6A-B and Figure S6A). We obtained similar results using OVA antigen instead of gluten (Figure S6B-C). Gluten proteins, predominantly gliadins in wheat, are resistant to complete degradation by mammalian enzymes, which results in the production of large peptides with immunogenic sequences such as the 33-mer in α-gliadin [45]. Certain intestinal bacteria participate in gliadin degradation including 33-mer gluten peptides, reducing their immunogenicity [46]. To assess whether *T. arnold* protects from LOT by reducing the immunogenicity of gluten peptides, we incubated *T. arnold* with chymotrypsin-digested gliadin to measure the amount of QPQLPQ-peptide, a key motif in the major immunogenic epitope within the 33-mer peptide [46]. Although *T. arnold* was metabolically active during *in vitro* co-culture with gliadin as observed by the production of succinate and active locomotion after 20 hours of *in vitro* culture (Figure S4C; Videos S1 and S2), it did not digest 33-mer gluten peptides in contrast to co-cultures of small intestinal contents of *T. arnold*-free mice (Figure 6C). Furthermore, a gluten-containing diet did not alter the abundance of *T. arnold* in the intestine when compared to a gluten-free diet, suggesting that gluten is not a major nutritional source for *T. arnold* in contrast to water-soluble fibers (Figure S6D and [28]). In addition to intestinal environmental conditions favoring Th1 cell responses against dietary antigen, transglutaminase-2 (TG2) activation is thought to promote CeD pathogenesis by increasing the affinity of gluten peptides for HLA-DQ2 and DQ8 molecules through posttranslational modifications [1–3]. T1L infection induces TG2 activation [15]. To test whether *T. arnold* suppresses T1L-mediated TG2 activation, we quantified the incorporation of 5-(biotinamido)-pentylamine (5BP), a small-molecule TG2 activity probe. We found that *T. arnold* effectively suppressed T1L-mediated TG2 activation (Figure 6D), suggesting that *T. arnold* prevents LOT and prevents the modification of gluten peptides.

Based on our findings about the protective role of *T. arnold* in a CeD mouse model, we hypothesized that protists of the *Parabasalia* family, including *Tritrichomonas* spp. and other human gut colonizing protists such as *Dientamoeba fragilis* and *Pentatrichomonas hominis* [26], could protect against LOT and CeD development in humans. To investigate a role for *Parabasalia* in CeD, we isolated DNA from stool samples of healthy individuals and those with active CeD and conducted ITS sequencing using *Parabasalia* specific primers [26]. We detected *Parabasalia* in 35% of controls (8/23) but only in 8% of active CeD patients (2/26) (Figure 6E), suggesting that *Parabasalia* are underrepresented in the intestines of persons with CeD compared with healthy controls. We detected *Parabasalia* with ITS sequence homology closest to *Pentatrichomonas hominis* and *Tritrichomonas* spp (Dataset S1). Further stratification of the detected strains showed that *Tritrichomonas* spp. was overrepresented in controls compared to CeD patients (Figure 6F), whereas *Pentatrichomonas hominis* was detected in one control and two CeD patients who were also positive for *Tritrichomonas* spp. (Figure 6G). Taken together, our findings that *T. arnold* prevented T1L-mediated abrogation of oral tolerance to gluten and T1L-mediated TG2 activation and that *Parabasalia* are underrepresented in CeD patients compared to controls, suggest that *T. arnold*-related strains may protect against LOT to gluten and development of CeD.

DISCUSSION

Besides the requirement for HLA DQ2 or DQ8, additional genetic and environmental factors are needed for the development of CeD [1]. Viruses have been implicated as a potential environmental trigger in CeD pathogenesis [11-14]. Concordantly, we discovered that reovirus strain T1L and murine norovirus strain CW3 promote LOT to dietary gluten [15,16]. In this study, we made the unexpected finding that an undescribed commensal *Tritrichomonas* species, *Tritrichomonas arnold* (*T. arnold*), protected against virus-mediated LOT by directly suppressing the virus-induced inflammatory program in dietary antigen-presenting cDC1, and this with neither impacting the viral host immune responses nor requiring the microbiota. Mechanistically, we showed that *T. arnold* restrains the reovirus-induced proinflammatory IRF1/NF-κB program of cDC1 and thus limit their ability to promote Th1 cell responses. Furthermore, we showed that *T. arnold* mediated protection from virus-induced LOT is not specific to T1L but was also observed with CW3. Collectively, our findings highlight the protective role of *T. arnold* against reovirus-mediated LOT to gluten and suggest a potentially protective role of *Parabasalia* against LOT events leading to CeD development in humans.

While succinate produced by *T. arnold* promoted mucosal type-2 immunity, it was insufficient to promote tolerance or protect against T1L-induced LOT, suggesting that *T. arnold* modulates immune responses to dietary antigens independent of succinate. Given its large genome size of approximately 100 megabases (unpublished findings), *T. arnold* likely harbors additional immunoregulatory functions besides succinate which are yet to be explored. In line with this hypothesis, our data suggest that metabolites secreted by *T. arnold* are sufficient to restrain T1L-mediated proinflammatory DC-mediated Th1 cell responses *ex vivo*.

While we showed that *T. arnold* directly acts on DCs to suppress the virus-induced inflammatory IRF1/NF-κb program in dietary antigen-presenting DCs, the mechanism of how *T. arnold* promotes tolerogenic DC responses during homeostasis remains undetermined. In this regard, the roles of Cdk19 and Dectin1, identified in our cDC1 RNA-seq, in *T. arnold*-mediated oral tolerance warrant further investigation. It is possible that the mechanisms by which *T. arnold* modulates dietary antigen-presenting DCs under homeostasis and enteric inflammation are uncoupled from each other. In line with this hypothesis, we showed that while *T. arnold* potently suppressed the T1L-induced inflammatory transcriptional profile in T1L-induced DCs, it failed to induce an obvious tolerogenic transcriptional gene profile during homeostasis. The evolutionary benefit for *T. arnold* to modulate tolerogenic responses to dietary antigens is unknown but may have evolved to evade unwanted immune responses to itself; however, this hypothesis warrants to be tested in future studies.

In contrast to a study that found *Dientamoeba fragilis* in up to 30% of individuals from a healthy cohort in Colombia, South America [26], we did not detect *Dientamoeba fragilis* in stool samples collected from patients attending the endoscopic clinic at McMaster University, Canada. It is not well understood how *Parabasalia* colonize the human gut and whether such colonization is persistent or intermittent. These parameters could contribute to

the geographically distinct human gut colonizing *Parabasalia* strains, hence providing further explanation of how environmental factors contribute to differences in CeD prevalence in otherwise genetically similar populations [1]. Furthermore, as shown in our and other mouse studies [28], differences in consumption of dietary components such as fibers may explain variation in colonization of *Parabasalia* strains and should be further explored. Interestingly, a population-based case-control study found that antibiotic use prior to CeD onset, especially metronidazole, which targets anaerobic microbes and is highly potent in eradicating gut protists, is associated with CeD development [47]. This observation is supported by our findings that mice depleted of *T. arnold* through dietary intervention failed to protect against T1L-mediated LOT (Figure 3H), further demonstrating that active colonization is sufficient and required to retain protection from virus-mediated LOT. One promising strategy to promote oral tolerance and prevent LOT or reinstate tolerance in CeD is to use the immunoregulatory potential of commensal gut microbes. Here, we identified an oral-tolerance-promoting protist that can prevent virus-mediated LOT to gluten in a CeD-relevant mouse model.

There is an unmet need to develop effective therapies to prevent LOT to gluten in at-risk individuals and to reinstate oral tolerance to gluten in CeD patients. Furthermore, the need for the development of an adjunct treatment to the gluten-free diet is supported by the difficulties in strictly excluding gluten from the diet and the lack of mucosal healing observed in 40% of adults with CeD who maintain a gluten-free diet. Our study will motivate a new line of investigation to use oral tolerance-promoting protists in CeD and potentially other immune-mediated food sensitivities including food allergies.

Limitations of the study

While data from murine models [48-50] support a role of Treg cells in oral tolerance and the suppression of unwanted Th1 cell responses towards dietary antigens, the OT-II T cell conversion and DTH assays used in this study provide an incomplete picture and may or may not recapitulate functional oral tolerance in humans. While we provide evidence for the presence of *Parabasalia* in a fraction of human stool samples, future studies are required to firmly define the *Parabasalid* species that colonize humans using next generation metagenomic sequencing approaches and larger cohort sizes. It is possible that other *Parabasalia* strains can promote oral tolerance and protect from virus-induced LOT. Furthermore, while we uncovered that *T. arnold*-derived metabolites are sufficient to suppress virus-induced proinflammatory DC responses, future studies will need to identify the specific metabolite(s) and the mechanisms in suppressing proinflammatory DCs. Additional studies should address whether *T. arnold* is able to reestablish oral tolerance to provide a potential therapeutic avenue for CeD and food allergy patients.

STAR * METHODS

RESOURCE AVAILABILITY

Lead contact—Further information and requests for resources and reagents should be directed to and will be fulfilled by the lead contact, Reinhard Hinterleitner (reinhard@pitt.edu).

Materials availability—Materials generated in this study are available from the lead contact upon request.

Data and code availability—Raw and processed RNA-seq data of mLN and mLN-derived DC1s are available at Gene Expression Omnibus (GSE230558; GSE230530). Remaining data needed to support the conclusion of this manuscript are included in the main text and supplementary materials. Any additional information required to reanalyze the data reported in this paper is available from the lead contact upon request. This paper does not report original code.

EXPERIMENTAL MODEL AND STUDY PARTICIPANT DETAILS

Human stool samples—Stool samples from consented healthy volunteers (controls) and patients with CeD were collected and processed in anaerobic conditions, frozen, and stored at −80°C until analysis at McMaster University. CeD diagnosis (n=26; age range: 19-75; 65% females) was based on a positive serology for anti-transglutaminase-2 (TG2) antibodies (IgA) or deamidated gliadin antibodies (IgG) and confirmed by duodenal biopsies, as assessed by a pathologist. Controls (n=23; age range:19-57; 55% females) had normal CeD serology and endoscopy and no functional gastrointestinal disorders (according to the Rome IV criteria). Subjects with concomitant inflammatory bowel disease or any other autoimmune disease were excluded. The sample collection was approved by the Hamilton Integrated Research Ethics Board (HiREB #12599-T for CeD patients; HiREB #2820 for controls).

Animals—All knockout and transgenic mice used in this study are on a C57BL/6 background. $RAG^{-/-}$ $OT\text{-}II^{+/-}$ $CD45.1^{+/+}$ mice were provided by Dr. Bana Jabri and bred and housed in our animal facility. HLA-DQ8 transgenic (DQ8tg) mice were described [15] and maintained on a gluten-free diet (AIN76A, Envigo). B6.129P2-$Il18^{tm1Aki}$/J (IL-18-deficient) mice and C57BL/6 (WT) mice were purchased from Jackson Laboratories. Female and male mice were used for experiments. Except for DQ8tg mice which were housed at the University of Chicago, all other mouse strains were housed at the University of Pittsburgh animal facility. In both locations mice were housed under specific pathogen-free (SPF) conditions, where cages were changed on a weekly basis; ventilated cages, bedding, food, and water (non-acidified) were autoclaved before use, ambient temperature maintained at 23°C, and 5% Clidox-S was used as a disinfectant. Experimental cages were randomly housed on two different racks in the vivarium and all cages were kept on automatic 12-h light/dark cycles. Germ-free C57BL/6 WT mice were maintained in flexible film isolators at the University of Pittsburgh Gnotobiotic facility. Animal husbandry for both SPF and germ-free facilities, and experimental procedures were conducted in accordance with Public Health Service policy and approved by the University of Pittsburgh and University of Chicago Institutional Animal Care and Use Committee.

METHOD DETAILS

Infection with reovirus and quantification of virus-specific antibody responses—Reovirus strain type 1 Lang (T1L) virions were purified using CsCl gradient centrifugation and viral titer determinations were conducted using plaque assays as

described [15]. Mice were inoculated perorally with purified 10^9 plaque-forming units (PFU) of T1L diluted in phosphate-buffered saline (PBS) using a 22-gauge round-tipped needle (Cadence Science). To assess T1L infection in the intestine, a 3 cm section of the ileum was resected, and viral titers were determined by plaque assay. Reovirus-specific antibody responses in sera were determined 18 days post T1L infection using a 60% plaque-reduction neutralization assay (PRNT 60) as described [15].

Infection with norovirus—Murine norovirus strain CW3 stocks were generated from plasmids as previously described [51]. Mice were inoculated perorally with purified $5x10^7$ PFU of CW3 diluted in PBS using a 22-gauge round-tipped needle (Cadence Science).

***Tritrichomonas* arnold isolation, colonization, and *in vitro* culture—**Cecal contents were harvested from *T. arnold* colonized C57BL/6 mice and mashed through a 100 μM cell strainer. Cecal contents were washed 3 times with PBS containing 0.5 μg/ml Amphotericin, 20 μg/ml Gentamicin, 100 μg/ml Streptomycin, 50 μg/ml Vancomycin and 100 U/ml Penicillin (Sigma) and centrifuged after each wash at 200g for 5 minutes. *T. arnold* was further purified by a 40% Percoll at 1000g for 15 minutes without braking. *T. arnold* was washed 3 times with sterile PBS to remove remaining antibiotics. The number and viability of isolated *T. arnold* was determined by counting with a hemocytometer. Approximately $1x10^6$ *T. arnold* in 200 μl PBS were orally gavaged into *Tritrichomonas*-free C57BL/6 mice. For germ-free experiments and *in vitro* cultures *T. arnold* was sorted twice on a BD Aria IIU (BD Biosciences) post Percoll purification based on size (forward scatter) to exclude any residual bacterial contaminants. For *in vitro* cultures, *T. arnold* was incubated anaerobically in glass vials at a 15-degree angle at 37°C in RPMI media containing 10% FBS for 4 – 24 hours.

***In-vivo* T cell conversion assay—**At the start of the experiment C57BL/6 mice were colonized with $1x10^6$ *T. arnold* in 200 μl PBS or PBS alone by oral gavage for 12 days. Naïve $CD4^+$ T cells were purified from the spleen and lymph nodes of $RAG^{-/-}$ OT-$II^{+/-}$ $CD45.1^{+/+}$ mice and sorted on a BD Aria IIU (BD Biosciences). Approximately, 10^5 OT-II T cells were transferred retro-orbitally into congenic C57BL/6 mice. 1 day post OT-II T cell transfer, mice were gavaged with 10^9 PFU T1L or $5x10^7$ PFU of CW3 in 200 μl PBS or PBS alone. Mice were fed an OVA-containing diet (ENVIGO, TD.130362, 10 mg/kg) for 6 days. For germ-free experiments, cellulose-containing diet experiments, and recombinant IL-25 treatment experiments, mice received OVA (grade V, Sigma) dissolved in the drinking water (1.5%) for 6 days.

***In vivo* succinate and recombinant IL-25 treatment—**C57BL/6 mice received 150 mM succinate in drinking water 12 days prior to *in vivo* T cell conversion assay for the duration of the experiment. C57BL/6 mice were subjected to daily intraperitoneal injections of 300 ng recombinant mouse IL-25 (in 100 μl sterile PBS) or PBS alone for 6 days as indicated.

Loss of tolerance and delayed type hypersensitivity assay—At the start of the experiment a subset of DQ8tg mice or WT were colonized with $1x10^6$ *T. arnold* in 200 μl PBS by oral gavage. 12 days post *T. arnold* administration, mice received a dose of 50 mg

of chymotrypsin-digested gliadin (CT-gliadin) or 50 mg OVA [15] by oral gavage for 2 days. In the course of the first CT-gliadin or OVA feeding, a subset of mice was gavaged with 10^9 PFU T1L. Two days after CT-gliadin or OVA administration and infection, a mixture of complete Freund's adjuvant (CFA, Sigma) and CT-gliadin or OVA was administered subcutaneously in the lower back as an emulsion of 100 μl CFA and 100 μl PBS containing 300 μg CT-gliadin or OVA, under isoflurane gas anesthesia. At day 27 or 35, mouse sera were obtained by submandibular bleeding for anti-gliadin or anti-OVA IgG2c enzyme-linked immunosorbent assay (ELISA) quantification. IgG2c ELISA was conducted as described [15]. Ear challenges were conducted 14 and 24 days after immunization. A volume of 20 μl of 100 μg CT-gliadin or OVA/ PBS was injected under isoflurane gas anesthesia. Ear thickness was measured 2 days after second CT-gliadin or OVA challenge using a digital precision caliper (Fisher Scientific). Swelling was determined by subtracting pre-challenge from post-challenge ear thickness.

DNA extraction from intestinal contents and feces for 28S RT-PCR—Total DNA was extracted using the Fast DNA Stool Mini Kit (Qiagen, 51604). For quantification, quantitative PCR of the 28S rRNA-encoding gene was conducted on a Bio-Rad CFX384 using iTaq™ SYBR (Bio-Rad, 1725125). *Tritrichomonas* 28S rRNA gene qPCR (28S GCTTTTGCAAGCTAGGTCCC; 18S TTTCTGATGGGGCGTACCAC) was normalized to the host murine *Ifnb1* gene [24,52].

Parabasalia internal transcribed spacer (ITS) sequencing—Total DNA was extracted from stool samples using the Fast DNA Stool Mini Kit (Qiagen, 51604). Separate processing areas for DNA extraction and PCR amplification for both human and mouse samples were used. For ITS sequencing of human stool samples, the ITS region was PCR-amplified using pan-parabasalid primers (28S CTTCAGTTCAGCGGGTCTTC; 18S AACCTGCCGTTGGATCAGT) described in [26]. For ITS sequencing of the *Tritrichomonas sp.* identified in the University of Pittsburgh vivarium we used pan-parabasalid primers (28S TCCTCCGCTTAATGAGATGC; 18S AATACGTCCCCTGCCCTTTGT) described in [25,26]. The resulting PCR products were purified from gels and submitted to Azenta Life Sciences for Sanger Sequencing and a BLASTn search was conducted. Alignment with the ITS sequences of *T. muris* (GenBank: AY886843.1), *T. musculis* (GenBank: KX000922.1), *T. rainier* (GenBank: MH370486.1), and *Tritrichomonas sp.* (GenBank: MF375342.1) was conducted [53,54].

RNA processing and RT-PCR—RNA was prepared using the RNeasy Mini Kit (Qiagen, 74136). cDNA synthesis was conducted using iScript™ (Bio-Rad, 1708891BUN) according to the manufacturer's instructions. Expression analysis was conducted in duplicate via RT–PCR on a Bio-Rad CFX384 using iTaq™ SYBR (Bio-Rad, 1725125). Expression levels were quantified and normalized to *Gapdh* expression. Murine *Gapdh, Il27*, and murine norovirus primers were previously described in [15].

Antibodies and flow cytometry—Single cell suspensions were pelleted and resuspended in FACS buffer (PBS, 2% FBS) for immunostaining and subsequent flow cytometry analysis. Cell suspensions were incubated with Fc Block (BD

Biosciences, 553142) before staining with fluorophore-conjugated monoclonal antibodies. All fluorophore-conjugated antibodies used are listed as follows (clone, fluorophore, company, catalog number): CD45.1 (A20, BV480, BD Biosciences, 746666), CD4 (GK1.5, BV650, BD Biosciences, 563232), I-A/I-E (M5/114.15.2, APC-Fire750, BioLegend, 107652), Foxp3 (FJK-16s, FITC, eBioscience, 11-5773-82), Tbet (4B10, APC, eBioscience, 17-5825-82), Gata3 (TWAJ, PerCPeF710, eBioscience, 46-9966-42), Rorγt (AFKJS-9, PE, eBioscience, 12-6988-82), IFNγ (XMG1.2, BV605, BioLegend, 505839), CD11b (M1/70, APCeF780, eBioscience, 47-0112-82), CD45 (30-F11, BV480, BD Biosciences, 566095), CD44 (IM7, APC, BD Biosciences, 559250), CD62L (MEL-14, PE, eBioscience, 12-0621-81), CD45 (30-F11, APC-R700, BD Biosciences, 565478), CD4 (GK1.5, BUV395, BD Biosciences, 563790), CD11b (M1/70, PEcy7, eBioscience, 25-0112-82), CD19 (1D3, BV605, BD Biosciences, 563148), CD3 (17A2, BV605, BD Biosciences, 564009), Ter119 (TER-119, BV605, BD Biosciences, 563323), IL-12p40 (C17.8, PE, eBioscience, 12-7123-82), CD86 (GL-1, AF647, BioLegend, 105020), CD11c (N418, BV421, BD Biosciences, 565452), CD103 (M290, BV786, BD Biosciences, 564322), F4-80 (BM8, PEcy5, eBioscience, 15-4801-82), I-A/I-E (M5/114.15.2, FITC, eBioscience, 11-5321-82), CD8a (53-6.7, BV570, BioLegend, 100740), I-A/I-E (M5/114.15.2, BV421, BioLegend, 107632), CD45 (30-F11, BUV395, BD Biosciences, 564279), CD11c (HL3, FITC, BD Biosciences, 557400), CD11b (M1/70, BV605, BioLegend, 101257), CD103 (M290, APC, BD Biosciences, 562772), CD8a (53-6.7, BUV737, BD Biosciences, 612759), IFNγ (XMG1.2, PEcy7, Tonbo Biosciences, 60-7311), CD45.2 (104, BUV615, BD Biosciences, 751642), KLRG1 (2F1, BV786, BD Biosciences, 565477), NK1.1 (PK136, BUV805 BD Biosciences, 741926). Zombie NIR Fixable Viability Kit was purchased from BioLegend (423106). Fixable Aqua Dead Cell Stain Kit was purchased from Life Technologies (L34966). CellTrace Violet Cell Proliferation Kit was purchased from Thermo Fisher Scientific (C34557) and used according to manufacturer's protocol. For analysis of transcription factors and cytokine expression cells were incubated in RPMI media in the presence of 50 ng/ml phorbol 12-myristate 13-acetate (PMA), 500 ng/ml ionomycin (Sigma), 1.3 μl/ml Golgi Stop and 1 μl/ml Golgi Plug (BD Biosciences) for 3 hours at 37°C, 5% CO_2. For intracellular staining cells were permeabilized with the Foxp3 fixation/permeabilization kit from eBioscience (00-5523-00). For IL-12p40 staining, cells were incubated in RPMI media in the presence of 1 μl/ml Golgi Plug for 6 hours at 37°C, 5% CO_2. For intracellular staining cells were permeabilized with the Cytofix/Cytoperm kit from BD Biosciences (554714). Flow cytometry analysis was conducted on a Cytek Aurora (Cytek). Cell sorting was conducted on a BD Aria IIU (BD Biosciences). Data was analyzed with FlowJo (Treestar).

Cell dissociation and isolation—Small intestinal and cecum draining mesenteric lymph nodes (mLN) and Peyer's Patches were dissected followed by digestion with 1 mg/ml collagenase VIII (Sigma) in a shaking incubator at 37°C, 220 rpm for 30 minutes. After the incubation, 10 μl/ml of 0.5 M EDTA (Fisher Scientific) was added to inactivate the collagenase and cells were mashed through a 100 μm cell strainer to obtain a single cell suspension.

Oral antigen uptake by DCs—OVA was labelled with Alexa Fluor-647 succinimidyl ester according to the manufacturer's protocol (Molecular Probes). *T. arnold* colonized mice or control mice received 3.2 mg OVA-Alexa Fluor-647 by oral gavage. Mice were euthanized 18 hours post-feeding and OVA uptake by DCs in mLN was assessed by flow cytometry.

***In vitro* T cell conversion assay—**mLN DCs were isolated and purified (CD11c Positive Selection Kit II, STEMCELL Technologies). $2x10^4$ DCs were co-cultured for 3 days with $5x10^4$ FACS sorted naïve OT-II $CD4^+$ T cells in the presence of 1 μg/ml OVA peptide (OVA323-339, Invivogen), 0.25 ng/ml TGFb (recombinant mouse TGF-b1, BioLegend), and 1:20 dilution of *T. arnold* culture supernatant from $1x10^6$ /ml *T. arnold* as indicated.

Analysis of cytokine production—IFNγ was measured using electrochemiluminescence (IFNg V-PLEX Mouse, Meso Scale Diagnostics).

QPQLPY-peptide quantification—1 mg/ml CT-gliadin was incubated with $1x10^6$/ml *T. arnold* or media only (negative control) anaerobically in glass vials at a 15-degree angle at 37°C in RPMI media containing 10% FBS for 4 and 18 hours. As positive control, small intestinal contents from SPF non-*T. arnold* colonized mice were diluted 1:4 in De Man, Rogosa and Sharpe (MRS) broth and incubated under anaerobic conditions at 37°C for 4 hours with 1 mg/ml CT-gliadin. Supernatants were collected and remaining amount of QPQLPY-peptide, a key motif in the major immunogenic epitope within the 33-mer peptide from α-gliadin was measured with the competitive G12 ELISA GlutenTox kit according to the manufacturer's instructions [55].

Measurement of butyrate and succinate by liquid chromatography high resolution-mass spectrometry (LC-HRMS)—Cecum samples were homogenized with 50% aqueous acetonitrile at a ratio of 15:1 μl/mg. 50 μL culture supernatants were diluted 1:1 in 100% acetonitrile and vortexed vigorously. 10 μM deuterated internal standard (D_5)-butyrate and (D_6)-succinate (CDN Isotopes) were added. Samples were homogenized using a FastPrep-24 system (MP-Bio), with Matrix D at 60hz for 30 seconds, before being cleared of protein by centrifugation at 16,000 x *g*. Cleared supernatants (60 μL) were collected and derivatized using 3-nitrophenylhydrazine. Each sample was mixed with 20 μL of 200 mM 3-nitrophenylhydrazine in 50% aqueous acetonitrile and 20 μL of 120 mM N-(3-dimethylaminopropyl)-N0-ethylcarbodiimide −6% pyridine solution in 50% aqueous acetonitrile. The mixture was incubated at 50°C for 40 minutes and the reaction was stopped with 0.45 mL of 50% aqueous acetonitrile. Derivatized samples were injected (5 μL) via a Thermo Vanquish UHPLC and separated over a reversed phase Phenomenex Kinetex 150 mm x 2.1 mm 1.7 μM particle C18 maintained at 55°C. For the 20-minute LC gradient, the mobile phase consisted of the following: solvent A (water/0.1% formic acid) and solvent B (acetonitrile/0.1% formic acid). The gradient was the following: 0-2 minutes 15% B, increasing to 60% B over 10 minutes, followed by an increase to 100% B over 1 minute and holding for 3 minutes. This was followed by an equilibration at initial conditions for 4 minutes. The Thermo ID-X tribrid mass spectrometer was operated in both positive ion

mode, scanning in ddMS^2 mode (2 μscans) from 75 to 1000 *m/z* at 120K resolution with an AGC target of 2e5 for full scan, 2e4 for MS^2 scans using HCD fragmentation at stepped collision energies (15,35,50). Spray voltage was set at 3.0 kV for positive mode and source gas parameters were 45 sheath gas, 12 auxiliary gas at 320°C, and 3 sweep gas. Calibration was conducted prior to analysis using the PierceTM FlexMix Ion Calibration Solutions (Thermo Fisher Scientific). Integrated peak areas were then extracted manually using Quan Browser (Thermo Fisher Xcalibur ver. 2.7). Butyrate and succinate are reported as area ratio of the analyte to the internal standard [56].

Histology for PAS (Periodic acid Schiff staining)—A 10 cm piece of the jejunum was removed, cut longitudinally, and pinned down onto wax. Tissue pieces were fixed in 4% paraformaldehyde (PFA, Fisher Scientific) for 3 hours at 4°C and dehydrated in 30% w/v sucrose overnight. Tissue sections were coiled into a Swiss roll, embedded in optimal cutting temperature (OCT) compound (Tissue-Tek) and stored at −80°C prior to sectioning. Sections were sliced to 8 μm on a cryostat (Leica CM 1950) and fixed in RT methanol (Sigma-Aldrich) for 2 minutes prior to PAS staining according to manufacturer's protocol (Sigma-Aldrich, 395B-1KT). Slides were digitized for representative section (Nikon 90i, 0.75 N.A. 20x objective and a Hamamatsu Flash 4.0 CMOS camera) and were quantified for goblet cells per villi or per 100 intestinal epithelial cells.

Immunofluorescence Staining—For Tuft cell staining, 8-10 μm Swiss roles were fixed in 4% PFA for 10 minutes at RT. Slides were washed in blocking buffer (1% w/v bovine serum albumin, 0.1% Tween20, 1x PBS) for 10 minutes at RT. Sections were surrounded using a hydrophobic barrier (PAP pen, Thermo-Fischer) and permeabilized by incubating tissue in permeabilization buffer (0.4% Tritonx100, 1% fetal bovine serum, 1x PBS) for 10 minutes at RT. Sections were then incubated with anti-mouse IgG DCAMKL1 antibody (Abcam, ab31704) in blocking buffer for 1 hour at RT, washed three times in PBS, and incubated with anti-rabbit IgG (H+L) antibody, Alexa Flour Plus 647 (Thermo Fisher Scientific, A32733) for 30 minutes at RT, and washed 3 times in PBS. Slides were incubated in blocking buffer for 30 minutes at RT prior to staining for epithelial cells by anti-mouse IgG2a CD326/Ep-CAM conjugated to Alexa-Fluor 488 (Biolegend, 118210) for 1 hour at RT, washed three times in PBS, counter stained with 500 ng/ml 4',6-Diamidino-2-Phenylindole, Dihydrochloride (DAPI, Thermofisher) for 5 minutes at RT, washed three times in PBS, and mounted in Fluoromount-G (Thermofisher). Slides were stored light protected at 4°C until digitized (Nikon Ti inverted microscope equipped with a Nikon A1 point scanning confocal scan head and a 1.40 N.A. 20x objective or Keyence BZX-810 Widefield microscope equipped with an 0.75 N.A. 20x objective). Tuft cells were quantified for tuft cells per villi.

Visualization and quantification of TG2 activity—At the start of the experiment DQ8tg mice were colonized with 10^6 *Tritrichomonas* in 200 μl PBS or PBS alone by oral gavage. 12 days post *T. arnold* administration mice were gavaged with 10^9 PFU T1L in 200 μl PBS or PBS alone. The *in vivo* TG2 enzymatic activity was assessed 18 hours post T1L infection. Six and three hours prior to euthanasia, mice were injected i.p. with 100 mg/kg 5-(biotinamido)-pentylamine (5-BP), a substrate for TG2 transamidation

activity, which was synthesized following a published protocol [57]. Jejunal pieces were collected and frozen in optimum cutting temperature (OCT) compound (Tissue-Tek). Frozen sections of 5 μm thickness were cut, fixed in 1% paraformaldehyde, and TG2 protein was visualized by staining with a rabbit polyclonal anti-TG2 antibody (custom produced by Pacific Immunology), followed by AF488-conjugated donkey anti-rabbit IgG antibody (Invitrogen, A32790). TG2 enzymatic activity was measured using 5-BP crosslinking and was visualized by costaining with AF594-conjugated streptavidin (Invitrogen, S32356). Images were acquired at 20x magnification using a Leica SP8 Laser Scanning Confocal microscope. TG2 activity was quantified by systematically taking two sections of the jejunum from each mouse, quantifying the 5-BP signal / TG2 protein signal on a per villi basis. The mean 5-BP signal / TG2 signal is shown for each mouse that was assessed.

RNA sequencing processing and data analysis—For RNA sequencing on bulk mLN, libraries were prepared using the Illumina TruSeq protocol and sequenced with paired-end 75 bp reads on an Illumina HiSeq. For RNA-sequencing on $CD103^+$ $CD11b^-$ $CD8a^+$ mLN DCs, 1,000 $CD103^+$ $CD11b^-$ $CD8a^+$ DCs were FACS sorted into a 96-well plate containing 12.5 μl of lysis buffer and cDNA was generated using the Takara Smart-Seq HT Kit (Takara, 634438) following manufactures instructions, with 15 cycles of cDNA amplification. Smart-Seq cDNA was assessed for quality on an Agilent Fragment Analyzer 5300 using the High sensitivity NGS kit (Agilent, DNF-474-1000). Samples that passed QC with full length cDNA proceeded to library preparation using Illumina Nextera DNA prep (Illumina, 20018705) with UDI indexes (Illumina, 20027214) added using 8 PCR cycles. Libraries were pooled and sequenced on an Illumina NextSeq 2000 using a P2 200 cycle flow cell (Illumina 20046812), 2x101bp, for an average of ~30 million reads per sample. Libraries were demultiplexed using the NextSeq 2000 Dragen server (v 1.4.1.39716) and BCL Convert (v3.9.3). Reads were aligned to mouse reference genome *mm10* (GRCm38). Raw FASTQ files were processed using kallisto (v0.46.0) to obtain abundances (TPM) as well as the counts [58]. Sleuth (v0.30.0), an R (v4.2.0)/ Bioconductor package was used to identify differentially expressed transcripts among the groups of interest. Genes with false discovery rate (FDR) <0.1 were considered as significant differentially expressed genes (DEGs). The volcano plots representing the DEGs were obtained using EnhancedVolcano (1.14.0) package in R. Heatmaps based on z scores and hierarchical clustering using the one minus Pearson correlation were generated using Morpheus (https://software.broadinstiute.org/morpheus). WebGestalt was used to perform enrichment analysis, www.webgestalt.org [59].

QUANTIFICATION AND STATISTICAL ANALYSIS

Mice were allocated to experimental groups based on their genotype and randomized within the given age-matched groups. Male and female mice were used. Because our mice were inbred and matched for age and sex, we always assumed similar variance between the different experimental groups. All experimental and control animals were littermates, and none were excluded from the analysis at the time of collection. Data were analyzed using paired or unpaired two-tailed Student's *t*-test for single comparisons. Ordinary one-way ANOVA analysis (equal standard deviations) or Brown-Forsythe and Welch ANOVA analysis was used for multiple comparisons. ANOVA analysis was followed by Tukey's,

Sidak's or Dunnett T3 post hoc tests. Fisher's exact test was used test significance of observed frequencies of *Parabasalia* in human stool samples. Figures and statistical analysis were generated using GraphPad Prism 8 (GraphPad Software). The statistical test used, and *P* values are indicated in each figure legend. *P* values of < 0.05 were considered statistically significant. **P* < 0.05, ***P* < 0.01, ****P* < 0.001 and *****P* < 0.0001. ns = not significant.

Supplementary Material

Refer to Web version on PubMed Central for supplementary material.

ACKNOWLEDGMENTS

We thank the *Unified Flow Core* in the Department of Immunology at the University of Pittsburgh for flow cytometry analysis and sorting, the Gnotobiotic Core Facility, and the Health Sciences Mass Spectrometry Core at the University of Pittsburgh for their service. We thank the clinical team at McMaster University. Model figures were created with BioRender. For DC RNA-seq, cDNA generation, library preparation and sequencing were performed by the University of Pittsburgh Health Science Sequencing Core at the UPMC Children's Hospital of Pittsburgh, Pittsburgh, PA, USA. Funding: Investigator Start-up Fund, Department of Immunology, University of Pittsburgh School of Medicine to M.M. and R.H.; The Global Grants for Gut Health, co-supported by Yakult and Nature Research to R.H.; NIH grants R01AI168478 and R21AI163721 to R.H.; NIH grant R01DK098435 to B.J. and T.S.D.; NIH grants R01DK130897 and R21CA259636 to M.M.; Melanoma Research Alliance award (820677) to M.M.; NIH grant R01AI30055 to A.P.W and T.J.N.; Austrian Marshall Plan Foundation fellowships to M.S. and C.E.; Tsinghua University and China Scholarship Council fellowship to Y.Z.; Institute for Infection, Inflammation, and Immunity in Children (i4Kids) grant to R.H. and T.S.D.; NIH T32AI089443 to L.M.S. and L.V.D.K.; NIH T32AI060525 to P.H.B.; PACER Catalytic Award to R.H.; NIH grant S10OD023402 to S.L.G.; Canadian Institutes of Health Research -Project grant 168840 to E.F.V.; Heinz Endowments to T.S.D.

INCLUSION AND DIVERSITY

One or more of the authors of this paper self-identifies as an unrepresented ethnic minority in their field of research or within their geographical location.

REFERENCES

1. Abadie V, Sollid LM, Barreiro LB, and Jabri B (2011). Integration of genetic and immunological insights into a model of celiac disease pathogenesis. Annu Rev Immunol 29, 493–525. 10.1146/annurev-immunol-040210-092915. [PubMed: 21219178]
2. Tjon JM, van Bergen J, and Koning F (2010). Celiac disease: how complicated can it get? Immunogenetics 62, 641–651. 10.1007/s00251-010-0465-9. [PubMed: 20661732]
3. Sollid LM, and Jabri B (2013). Triggers and drivers of autoimmunity: lessons from coeliac disease. Nat Rev Immunol 13, 294–302. 10.1038/nri3407. [PubMed: 23493116]
4. Green PH, and Jabri B (2003). Coeliac disease. Lancet 362, 383–391. 10.1016/S0140-6736(03)14027-5. [PubMed: 12907013]
5. Rubio-Tapia A, Barton SH, and Murray JA (2011). Celiac disease and persistent symptoms. Clin Gastroenterol Hepatol 9, 13–17; quiz e18. 10.1016/j.cgh.2010.07.014. [PubMed: 20692372]
6. Nilsen EM, Jahnsen FL, Lundin KE, Johansen FE, Fausa O, Sollid LM, Jahnsen J, Scott H, and Brandtzaeg P (1998). Gluten induces an intestinal cytokine response strongly dominated by interferon gamma in patients with celiac disease. Gastroenterology 115, 551–563. 10.1016/s0016-5085(98)70134-9. [PubMed: 9721152]
7. Jabri B, and Sollid LM (2009). Tissue-mediated control of immunopathology in coeliac disease. Nat Rev Immunol 9, 858–870. 10.1038/nri2670. [PubMed: 19935805]
8. Esterhazy D, Loschko J, London M, Jove V, Oliveira TY, and Mucida D (2016). Classical dendritic cells are required for dietary antigen-mediated induction of peripheral T(reg) cells and tolerance. Nat Immunol 17, 545–555. 10.1038/ni.3408. [PubMed: 27019226]

9. Hinterleitner R, and Jabri B (2016). A dendritic cell subset designed for oral tolerance. Nat Immunol 17, 474–476. 10.1038/ni.3435. [PubMed: 27092796]
10. Raki M, Tollefsen S, Molberg O, Lundin KE, Sollid LM, and Jahnsen FL (2006). A unique dendritic cell subset accumulates in the celiac lesion and efficiently activates gluten-reactive T cells. Gastroenterology 131, 428–438. 10.1053/j.gastro.2006.06.002. [PubMed: 16890596]
11. Plot L, and Amital H (2009). Infectious associations of Celiac disease. Autoimmun Rev 8, 316–319. 10.1016/j.autrev.2008.10.001. [PubMed: 18973831]
12. Smits SL, van Leeuwen M, van der Eijk AA, Fraaij PL, Escher JC, Simon JH, and Osterhaus AD (2010). Human astrovirus infection in a patient with new-onset celiac disease. J Clin Microbiol 48, 3416–3418. 10.1128/JCM.01164-10. [PubMed: 20573860]
13. Stene LC, Honeyman MC, Hoffenberg EJ, Haas JE, Sokol RJ, Emery L, Taki I, Norris JM, Erlich HA, Eisenbarth GS, and Rewers M (2006). Rotavirus infection frequency and risk of celiac disease autoimmunity in early childhood: a longitudinal study. Am J Gastroenterol 101, 2333–2340. 10.1111/j.1572-0241.2006.00741.x. [PubMed: 17032199]
14. Troncone R, and Auricchio S (2007). Rotavirus and celiac disease: clues to the pathogenesis and perspectives on prevention. J Pediatr Gastroenterol Nutr 44, 527–528. 10.1097/MPG.0b013e31804ca0ec. [PubMed: 17460483]
15. Bouziat R, Hinterleitner R, Brown JJ, Stencel-Baerenwald JE, Ikizler M, Mayassi T, Meisel M, Kim SM, Discepolo V, Pruijssers AJ, et al. (2017). Reovirus infection triggers inflammatory responses to dietary antigens and development of celiac disease. Science 356, 44–50. 10.1126/science.aah5298. [PubMed: 28386004]
16. Bouziat R, Biering SB, Kouame E, Sangani KA, Kang S, Ernest JD, Varma M, Brown JJ, Urbanek K, Dermody TS, et al. (2018). Murine Norovirus Infection Induces TH1 Inflammatory Responses to Dietary Antigens. Cell Host Microbe 24, 677–688 e675. 10.1016/j.chom.2018.10.004. [PubMed: 30392830]
17. Siller M, Zeng Y, and Hinterleitner R (2020). Can Microbes Boost Tregs to Suppress Food Sensitivities? Trends Immunol 41, 967–971. 10.1016/j.it.2020.09.005. [PubMed: 33036909]
18. Caminero A, Meisel M, Jabri B, and Verdu EF (2019). Mechanisms by which gut microorganisms influence food sensitivities. Nat Rev Gastroenterol Hepatol 16, 7–18. 10.1038/s41575-018-0064-z. [PubMed: 30214038]
19. Constante M, Libertucci J, Galipeau HJ, Szamosi JC, Rueda G, Miranda PM, Pinto-Sanchez MI, Southward CM, Rossi L, Fontes ME, et al. (2022). Biogeographic Variation and Functional Pathways of the Gut Microbiota in Celiac Disease. Gastroenterology 163, 1351–1363 e1315. 10.1053/j.gastro.2022.06.088. [PubMed: 35810781]
20. Dobell C. (1920). The Discovery of the Intestinal Protozoa of Man. Proc R Soc Med 13, 1–15.
21. Adam RD (2001). Biology of Giardia lamblia. Clin Microbiol Rev 14, 447–475. 10.1128/CMR.14.3.447-475.2001. [PubMed: 11432808]
22. Stauffer W, and Ravdin JI (2003). Entamoeba histolytica: an update. Curr Opin Infect Dis 16, 479–485. 10.1097/00001432-200310000-00016. [PubMed: 14502002]
23. Yao C, and Koster LS (2015). Tritrichomonas foetus infection, a cause of chronic diarrhea in the domestic cat. Vet Res 46, 35. 10.1186/s13567-015-0169-0. [PubMed: 25880025]
24. Howitt MR, Lavoie S, Michaud M, Blum AM, Tran SV, Weinstock JV, Gallini CA, Redding K, Margolskee RF, Osborne LC, et al. (2016). Tuft cells, taste-chemosensory cells, orchestrate parasite type 2 immunity in the gut. Science 351, 1329–1333. 10.1126/science.aaf1648. [PubMed: 26847546]
25. Nadjsombati MS, McGinty JW, Lyons-Cohen MR, Jaffe JB, DiPeso L, Schneider C, Miller CN, Pollack JL, Nagana Gowda GA, Fontana MF, et al. (2018). Detection of Succinate by Intestinal Tuft Cells Triggers a Type 2 Innate Immune Circuit. Immunity 49, 33–41 e37. 10.1016/j.immuni.2018.06.016. [PubMed: 30021144]
26. Chudnovskiy A, Mortha A, Kana V, Kennard A, Ramirez JD, Rahman A, Remark R, Mogno I, Ng R, Gnjatic S, et al. (2016). Host-Protozoan Interactions Protect from Mucosal Infections through Activation of the Inflammasome. Cell 167, 444–456 e414. 10.1016/j.cell.2016.08.076. [PubMed: 27716507]

27. Escalante NK, Lemire P, Cruz Tleugabulova M, Prescott D, Mortha A, Streutker CJ, Girardin SE, Philpott DJ, and Mallevaey T (2016). The common mouse protozoa Tritrichomonas muris alters mucosal T cell homeostasis and colitis susceptibility. J Exp Med 213, 2841–2850. 10.1084/jem.20161776. [PubMed: 27836928]
28. Schneider C, O'Leary CE, von Moltke J, Liang HE, Ang QY, Turnbaugh PJ, Radhakrishnan S, Pellizzon M, Ma A, and Locksley RM (2018). A Metabolite-Triggered Tuft Cell-ILC2 Circuit Drives Small Intestinal Remodeling. Cell 174, 271–284 e214. 10.1016/j.cell.2018.05.014. [PubMed: 29887373]
29. Pabst O, and Mowat AM (2012). Oral tolerance to food protein. Mucosal Immunol 5, 232–239. 10.1038/mi.2012.4. [PubMed: 22318493]
30. Esterhazy D, Canesso MCC, Mesin L, Muller PA, de Castro TBR, Lockhart A, ElJalby M, Faria AMC, and Mucida D (2019). Compartmentalized gut lymph node drainage dictates adaptive immune responses. Nature 569, 126–130. 10.1038/s41586-019-1125-3. [PubMed: 30988509]
31. von Moltke J, Ji M, Liang HE, and Locksley RM (2016). Tuft-cell-derived IL-25 regulates an intestinal ILC2-epithelial response circuit. Nature 529, 221–225. 10.1038/nature16161. [PubMed: 26675736]
32. Gerbe F, Sidot E, Smyth DJ, Ohmoto M, Matsumoto I, Dardalhon V, Cesses P, Garnier L, Pouzolles M, Brulin B, et al. (2016). Intestinal epithelial tuft cells initiate type 2 mucosal immunity to helminth parasites. Nature 529, 226–230. 10.1038/nature16527. [PubMed: 26762460]
33. Arpaia N, Campbell C, Fan X, Dikiy S, van der Veeken J, deRoos P, Liu H, Cross JR, Pfeffer K, Coffer PJ, and Rudensky AY (2013). Metabolites produced by commensal bacteria promote peripheral regulatory T-cell generation. Nature 504, 451–455. 10.1038/nature12726. [PubMed: 24226773]
34. Lei W, Ren W, Ohmoto M, Urban JF Jr., Matsumoto I, Margolskee RF, and Jiang P (2018). Activation of intestinal tuft cell-expressed Sucnr1 triggers type 2 immunity in the mouse small intestine. Proc Natl Acad Sci U S A 115, 5552–5557. 10.1073/pnas.1720758115. [PubMed: 29735652]
35. McDole JR, Wheeler LW, McDonald KG, Wang B, Konjufca V, Knoop KA, Newberry RD, and Miller MJ (2012). Goblet cells deliver luminal antigen to CD103+ dendritic cells in the small intestine. Nature 483, 345–349. 10.1038/nature10863. [PubMed: 22422267]
36. Kulkarni DH, Gustafsson JK, Knoop KA, McDonald KG, Bidani SS, Davis JE, Floyd AN, Hogan SP, Hsieh CS, and Newberry RD (2019). Goblet cell associated antigen passages support the induction and maintenance of oral tolerance. Mucosal Immunol. 10.1038/s41385-019-0240-7.
37. Saenz SA, Siracusa MC, Monticelli LA, Ziegler CG, Kim BS, Brestoff JR, Peterson LW, Wherry EJ, Goldrath AW, Bhandoola A, and Artis D (2013). IL-25 simultaneously elicits distinct populations of innate lymphoid cells and multipotent progenitor type 2 (MPPtype2) cells. J Exp Med 210, 1823–1837. 10.1084/jem.20122332. [PubMed: 23960191]
38. Fleeton MN, Contractor N, Leon F, Wetzel JD, Dermody TS, and Kelsall BL (2004). Peyer's patch dendritic cells process viral antigen from apoptotic epithelial cells in the intestine of reovirus-infected mice. J Exp Med 200, 235–245. 10.1084/jem.20041132. [PubMed: 15263030]
39. Coombes JL, Siddiqui KR, Arancibia-Carcamo CV, Hall J, Sun CM, Belkaid Y, and Powrie F (2007). A functionally specialized population of mucosal CD103+ DCs induces Foxp3+ regulatory T cells via a TGF-beta and retinoic acid-dependent mechanism. J Exp Med 204, 1757–1764. 10.1084/jem.20070590. [PubMed: 17620361]
40. Luda KM, Joeris T, Persson EK, Rivollier A, Demiri M, Sitnik KM, Pool L, Holm JB, Melo-Gonzalez F, Richter L, et al. (2016). IRF8 Transcription-Factor-Dependent Classical Dendritic Cells Are Essential for Intestinal T Cell Homeostasis. Immunity 44, 860–874. 10.1016/j.immuni.2016.02.008. [PubMed: 27067057]
41. Martinez-Lopez M, Iborra S, Conde-Garrosa R, and Sancho D (2015). Batf3-dependent CD103+ dendritic cells are major producers of IL-12 that drive local Th1 immunity against Leishmania major infection in mice. Eur J Immunol 45, 119–129. 10.1002/eji.201444651. [PubMed: 25312824]
42. Ghislat G, Cheema AS, Baudoin E, Verthuy C, Ballester PJ, Crozat K, Attaf N, Dong C, Milpied P, Malissen B, et al. (2021). NF-kappaB-dependent IRF1 activation programs cDC1 dendritic cells to drive antitumor immunity. Sci Immunol 6. 10.1126/sciimmunol.abg3570.

43. Johannessen L, Sundberg TB, O'Connell DJ, Kolde R, Berstler J, Billings KJ, Khor B, Seashore-Ludlow B, Fassl A, Russell CN, et al. (2017). Small-molecule studies identify CDK8 as a regulator of IL-10 in myeloid cells. Nat Chem Biol 13, 1102–1108. 10.1038/nchembio.2458. [PubMed: 28805801]
44. Tang C, Kamiya T, Liu Y, Kadoki M, Kakuta S, Oshima K, Hattori M, Takeshita K, Kanai T, Saijo S, et al. (2015). Inhibition of Dectin-1 Signaling Ameliorates Colitis by Inducing Lactobacillus-Mediated Regulatory T Cell Expansion in the Intestine. Cell Host Microbe 18, 183–197. 10.1016/j.chom.2015.07.003. [PubMed: 26269954]
45. Shan L, Molberg O, Parrot I, Hausch F, Filiz F, Gray GM, Sollid LM, and Khosla C (2002). Structural basis for gluten intolerance in celiac sprue. Science 297, 2275–2279. 10.1126/science.1074129. [PubMed: 12351792]
46. Caminero A, Galipeau HJ, McCarville JL, Johnston CW, Bernier SP, Russell AK, Jury J, Herran AR, Casqueiro J, Tye-Din JA, et al. (2016). Duodenal Bacteria From Patients With Celiac Disease and Healthy Subjects Distinctly Affect Gluten Breakdown and Immunogenicity. Gastroenterology 151, 670–683. 10.1053/j.gastro.2016.06.041. [PubMed: 27373514]
47. Marild K, Ye W, Lebwohl B, Green PH, Blaser MJ, Card T, and Ludvigsson JF (2013). Antibiotic exposure and the development of coeliac disease: a nationwide case-control study. BMC Gastroenterol 13, 109. 10.1186/1471-230X-13-109. [PubMed: 23834758]
48. Hadis U, Wahl B, Schulz O, Hardtke-Wolenski M, Schippers A, Wagner N, Muller W, Sparwasser T, Forster R, and Pabst O (2011). Intestinal tolerance requires gut homing and expansion of FoxP3+ regulatory T cells in the lamina propria. Immunity 34, 237–246. 10.1016/j.immuni.2011.01.016. [PubMed: 21333554]
49. Kim KS, Hong SW, Han D, Yi J, Jung J, Yang BG, Lee JY, Lee M, and Surh CD (2016). Dietary antigens limit mucosal immunity by inducing regulatory T cells in the small intestine. Science 351, 858–863. 10.1126/science.aac5560. [PubMed: 26822607]
50. Hong SW, Krueger PD, Osum KC, Dileepan T, Herman A, Mueller DL, and Jenkins MK (2022). Immune tolerance of food is mediated by layers of CD4(+) T cell dysfunction. Nature 607, 762–768. 10.1038/s41586-022-04916-6. [PubMed: 35794484]
51. Van Winkle JA, Robinson BA, Peters AM, Li L, Nouboussi RV, Mack M, and Nice TJ (2018). Persistence of Systemic Murine Norovirus Is Maintained by Inflammatory Recruitment of Susceptible Myeloid Cells. Cell Host Microbe 24, 665–676 e664. 10.1016/j.chom.2018.10.003. [PubMed: 30392829]
52. Meisel M, Hinterleitner R, Pacis A, Chen L, Earley ZM, Mayassi T, Pierre JF, Ernest JD, Galipeau HJ, Thuille N, et al. (2018). Microbial signals drive pre-leukaemic myeloproliferation in a Tet2-deficient host. Nature 557, 580–584. 10.1038/s41586-018-0125-z. [PubMed: 29769727]
53. Di Tommaso P, Moretti S, Xenarios I, Orobitg M, Montanyola A, Chang JM, Taly JF, and Notredame C (2011). T-Coffee: a web server for the multiple sequence alignment of protein and RNA sequences using structural information and homology extension. Nucleic Acids Res 39, W13–17. 10.1093/nar/gkr245. [PubMed: 21558174]
54. Notredame C, Higgins DG, and Heringa J (2000). T-Coffee: A novel method for fast and accurate multiple sequence alignment. J Mol Biol 302, 205–217. 10.1006/jmbi.2000.4042. [PubMed: 10964570]
55. Caminero A, McCarville JL, Galipeau HJ, Deraison C, Bernier SP, Constante M, Rolland C, Meisel M, Murray JA, Yu XB, et al. (2019). Duodenal bacterial proteolytic activity determines sensitivity to dietary antigen through protease-activated receptor-2. Nat Commun 10, 1198. 10.1038/s41467-019-09037-9. [PubMed: 30867416]
56. Han J, Lin K, Sequeira C, and Borchers CH (2015). An isotope-labeled chemical derivatization method for the quantitation of short-chain fatty acids in human feces by liquid chromatography-tandem mass spectrometry. Anal Chim Acta 854, 86–94. 10.1016/j.aca.2014.11.015. [PubMed: 25479871]
57. DiRaimondo TR, Klock C, Warburton R, Herrera Z, Penumatsa K, Toksoz D, Hill N, Khosla C, and Fanburg B (2014). Elevated transglutaminase 2 activity is associated with hypoxia-induced experimental pulmonary hypertension in mice. ACS Chem Biol 9, 266–275. 10.1021/cb4006408. [PubMed: 24152195]

58. Bray NL, Pimentel H, Melsted P, and Pachter L (2016). Near-optimal probabilistic RNA-seq quantification. Nature Biotechnology 34, 525–527. 10.1038/nbt.3519.

59. Liao Y, Wang J, Jaehnig EJ, Shi Z, and Zhang B (2019). WebGestalt 2019: gene set analysis toolkit with revamped UIs and APIs. Nucleic Acids Res 47, W199–W205. 10.1093/nar/gkz401. [PubMed: 31114916]

HIGHLIGHTS

- *T. arnold* promotes oral tolerance and protects against virus-mediated LOT.
- *T. arnold* mediated protection is independent of antiviral immunity and the microbiota.
- Succinate and IL-25 are not sufficient to protect against virus-mediated LOT.
- *T. arnold* restrains virus-induced IRF1/NF-κB inflammatory responses in cDC1.

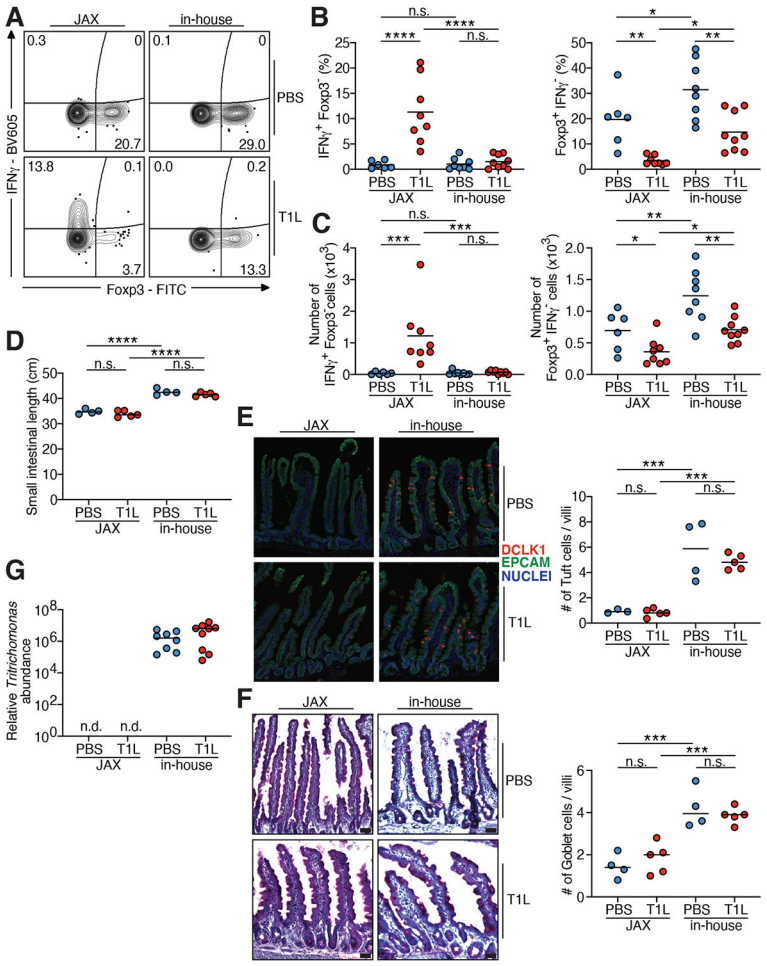

Figure 1. Suppression of T1L-induced LOT is associated with the presence of *Tritrichomonas* in in-housed mice.

(A-C) OT-II T cell conversion assay; see schematic in Figure S1A. Expression of Foxp3 and IFNγ in transferred OT-II T cells in the mLN assessed by flow cytometry. **(A)** Representative contour plots, **(B)** percentages and **(C)** absolute numbers. **(D)** Small intestine length **(E)** Tuft cells in the jejunum visualized by expression of DCLK1 in red; epithelial cells (EPCAM) in green; nuclei (DAPI) in blue. **(F)** Goblet cells in the jejunum visualized by PAS staining. **(E-F)** Representative images (left), quantification (right); Scale bars, 50 μm. **(G)** *Tritrichomonas* colonization in the cecum quantified by real time (RT)-PCR. Center is median. n.d. not detected. **(A-G)** Data represent two independent experiments (n=4-8 mice/group). **(A-F)** Center is mean, one-way ANOVA, Sidak's post hoc test. *$P < 0.05$, **$P < 0.01$, ***$P < 0.001$, ****$P < 0.0001$, n.s. not significant.

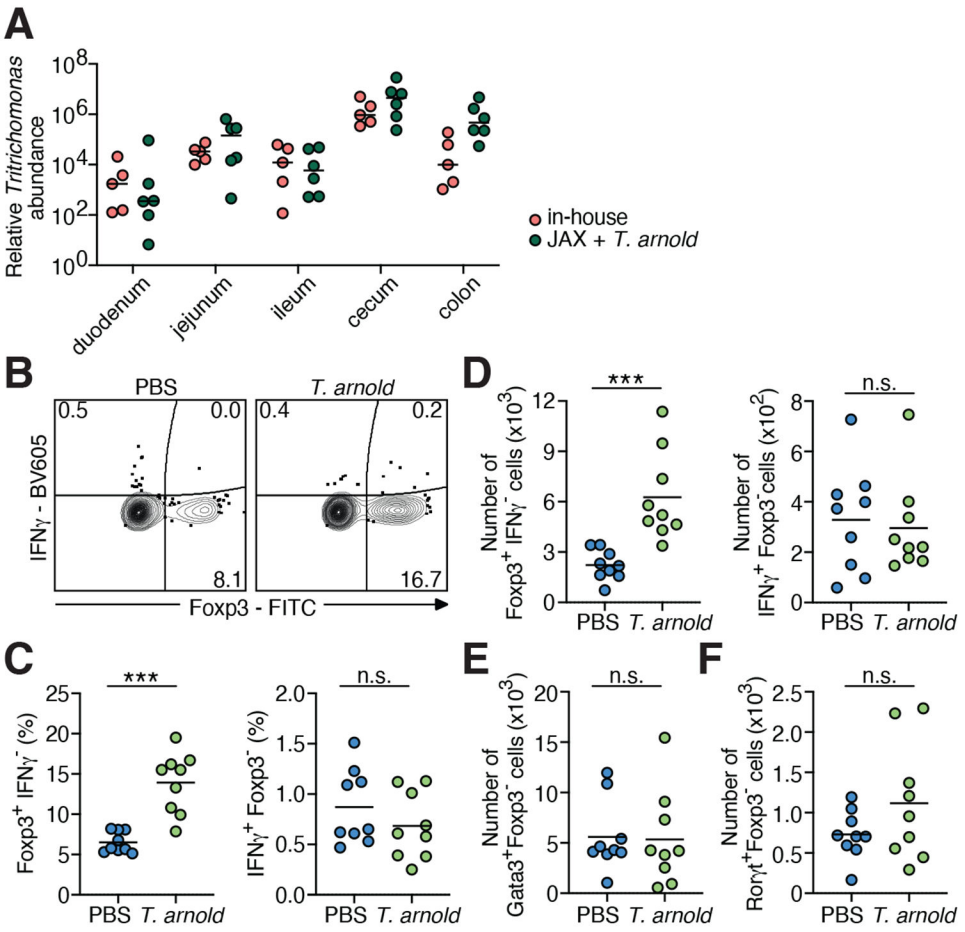

Figure 2. *T. arnold* promotes dietary antigen-specific Treg cell responses.

(A) WT mice were inoculated perorally with *T. arnold* for 12 days. *T. arnold* colonization quantified by RT-PCR from intestinal contents of different regions. Center is median. **(B-F)** OT-II T cell conversion assay; see schematic in Figure S2D. Expression of **(B-D)** Foxp3 and IFNγ, **(E)** Gata3, and **(F)** Rorγt in transferred OT-II T cells in the mLN assessed by flow cytometry. **(B)** Representative contour plots, **(C)** percentages and **(D-F)** absolute numbers. **(A-F)** Data represent two independent experiments (n=5-9 mice/group). **(C-F)** Center is mean, two-tailed unpaired *t*-test. ***$P < 0.001$, n.s. not significant.

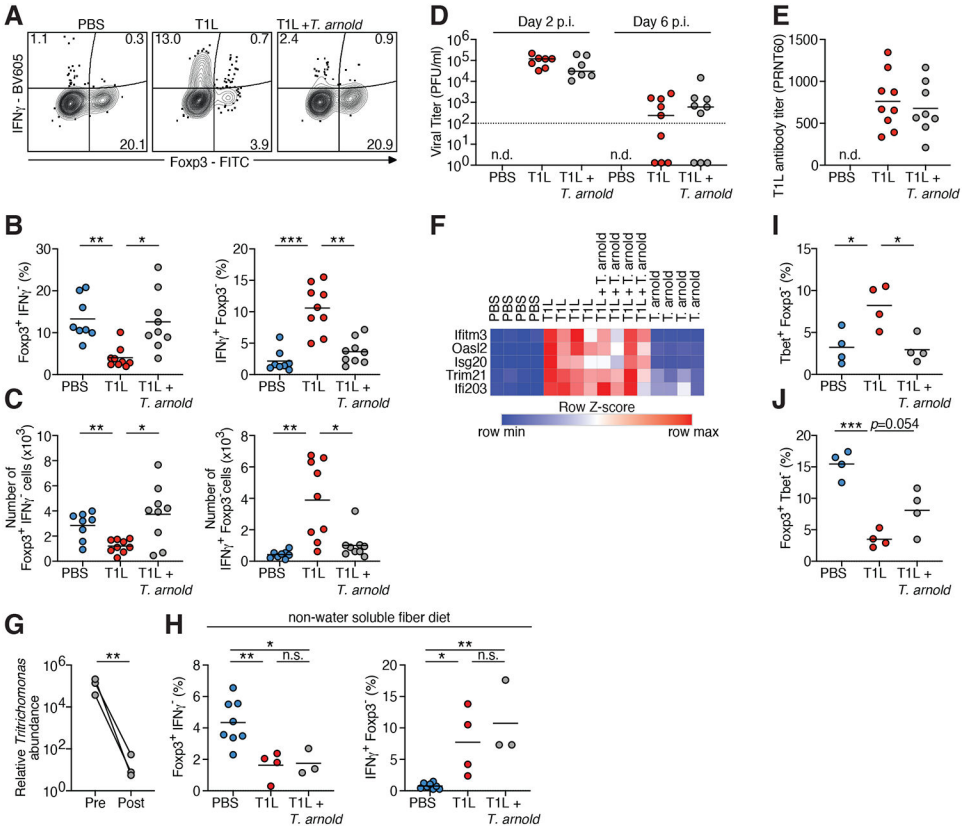

Figure 3. *T. arnold* protects against T1L-mediated LOT without impacting antiviral immunity and independent of the microbiota.

(A-F) OT-II T cell conversion assay; see schematic in Figure S3A. **(A-C)** Expression of Foxp3 and IFNγ in transferred OT-II T cells in the mLN assessed by flow cytometry. **(A)** Representative contour plots, **(B)** percentages and **(C)** absolute numbers. **(D)** T1L titers in the ileum assessed by plaque assay (post infection p.i.) (Plaque-forming unit (PFU)). Dotted line indicates detection limit. **(E)** 18 days post T1L infection sera were used for a plaque-reduction neutralization assay (PRNT 60). **(D-E)** Center is median. n.d. not detected. **(F)** RNA-seq of mLN 48 hours post T1L infection. Heat map of selected type-1 interferon inducible genes. The scale represents the Row Z-score. (n=4 mice/group). **(G)** *T. arnold* colonized mice were fed a non-water-soluble fiber diet for 4 weeks. *T. arnold* colonization quantified by RT-PCR from feces before (pre) and after (post) diet intervention. Lines connect values obtained from same mouse sampled pre and post diet intervention. Two-tailed paired *t*-test. **(H)** *T. arnold* colonized WT mice and control mice were fed non-water soluble fiber diet for 4 weeks prior to OT-II T cell transfer. One day after transfer mice were inoculated perorally with T1L or PBS and fed OVA in drinking water for 6 days. The expression of Foxp3 and IFNγ in transferred OT-II T cells in the mLN assessed by flow cytometry. Percentages are shown. **(I-J)** Germ-free WT mice were inoculated perorally with *T. arnold* or PBS for 12 days prior to OT-II T cell transfer. One day after transfer mice were inoculated perorally with T1L or PBS and fed OVA in drinking water for 6 days. The expression of **(I)** Tbet and **(J)** Foxp3 in transferred OT-II T cells in the mLN assessed by flow cytometry. Percentages are shown. **(B-E, H-J)** Data represent two independent

experiments (n=3-9 mice/group). **(B-C, I-J, H)** Center is mean, one-way ANOVA, Sidak's post hoc test. *$P < 0.05$, **$P < 0.01$, ***$P < 0.001$, n.s. not significant.

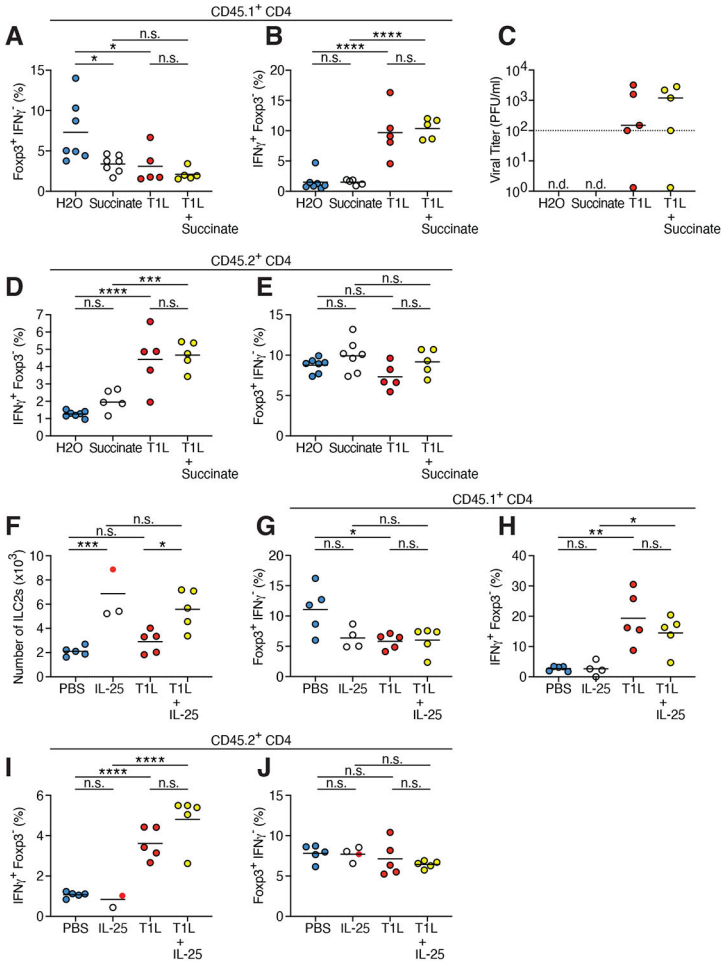

Figure 4. Succinate and IL-25 are not sufficient to protect against T1L-mediated LOT.

(A-E) OT-II T cell conversion assay; see schematic in Figure S4F. **(A-B, D-E)** The expression of Foxp3 and IFNγ in **(A-B)** transferred OT-II T cells **(D-E)** host CD4$^+$ T cells in the mLN assessed by flow cytometry. Percentages are shown. **(C)** T1L titers in the ileum assessed by plaque assay 6 days post infection (Plaque-forming unit (PFU)). Dotted line indicates detection limit. . n.d. not detected. **(F-J)** OT-II T cell conversion assay; see schematic in Figure S4G. **(F)** Absolute numbers of ILC2 in the mLN. **(G-J)** Expression of Foxp3 and IFNγ in **(G-H)** transferred OT-II T cells **(I-J)** host CD4$^+$ T cells in the mLN assessed by means of flow cytometry. Percentages are shown. **(A-J)** Data represent two independent experiments (n=4-7 mice/group). **(A-B, D-J)** Center is mean, one-way ANOVA, Sidak's post hoc test. **(C)** Center is median. *$P < 0.05$, **$P < 0.01$, ***$P < 0.001$, ****$P < 0.0001$, n.s. not significant.

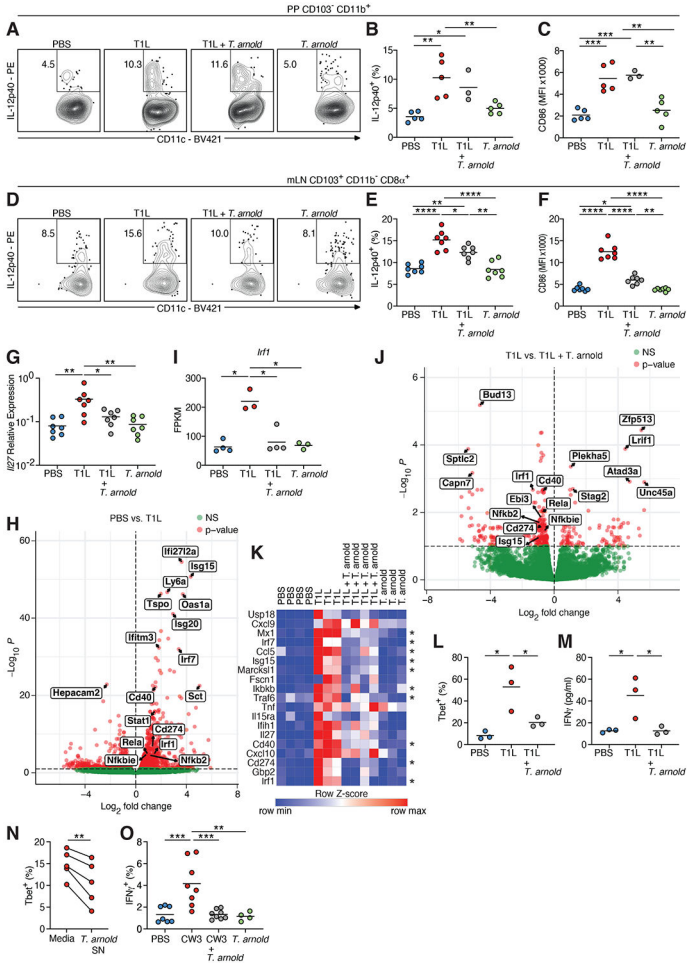

Figure 5. *T. arnold* restrains the virus-mediated proinflammatory program in dietary antigen-presenting DCs.

(A-M) WT mice were inoculated perorally with *T. arnold* or PBS for 12 days followed by peroral inoculation with T1L or PBS for 48 hours. **(A-F)** Expression of **(A-B, D-E)** IL-12p40 and **(C, F)** CD86 on **(A-C)** gated MHC-II^{+} CD11c^{+} CD103^{-} CD11b^{+} PP DCs and **(D-F)** gated MHC-II^{+} CD11c^{+} CD103^{+} CD11b^{-} CD8a^{+} mLN DCs assessed by flow cytometry. **(A, D)** Representative dot plots, **(B, E)** percentages, and **(C, F)** MFI. **(G)** *Il27* gene expression in the mLN quantified by RT-PCR. **(H-K)** RNA-seq of MHC-II^{+} CD11c^{+} CD103^{+} CD11b^{-} CD8a^{+} mLN DCs (n =3-4 mice/group). **(H)** Volcano blot for PBS vs T1L. **(I)** Normalized count number of *Irf1*. **(J)** Volcano blot for T1L vs T1L + *T. arnold*. **(K)** Heatmap showing IRF1 and NF-κB dependent DEGs increased in T1L compared to PBS. * Indicate significant differences between T1L vs T1L + *T. arnold* based on false discovery rate < 0.1. **(L-M)** mLN DCs co-cultured with naïve OT-II T cells for 3 days in presence of OVA peptide. **(L)** Expression of Tbet in OT-II T cells assessed by flow cytometry. **(M)** IFNγ in co-culture supernatants assessed by electrochemiluminescence (n=3 mice/group). **(N)** mLN DCs were pre-incubated with *T. arnold* culture supernatant and OVA peptide for 5 hours followed by co-culture with naïve OT-II T cells for 3 days. Expression of Tbet in OT-II T cells assessed by flow cytometry. Lines connect same mouse in the presence or absence of *T. arnold* supernatant (*T. arnold* SN). Two-tailed paired *t*-test. **(O)**

OT-II T cell conversion assay; see schematic in Figure S3A. Mice were inoculated perorally with CW3 or PBS instead of T1L. Expression of IFNγ in transferred OT-II T cells in the mLN assessed by means of flow cytometry. Percentages are shown. **(A-G, N-O)** Data represent two independent experiments (n=4-8 mice/group). **(A-G, I, L-M, O)** Center is mean, one-way ANOVA, Tukey's post hoc test. *$P < 0.05$, **$P < 0.01$, ***$P < 0.001$, ****$P < 0.0001$.

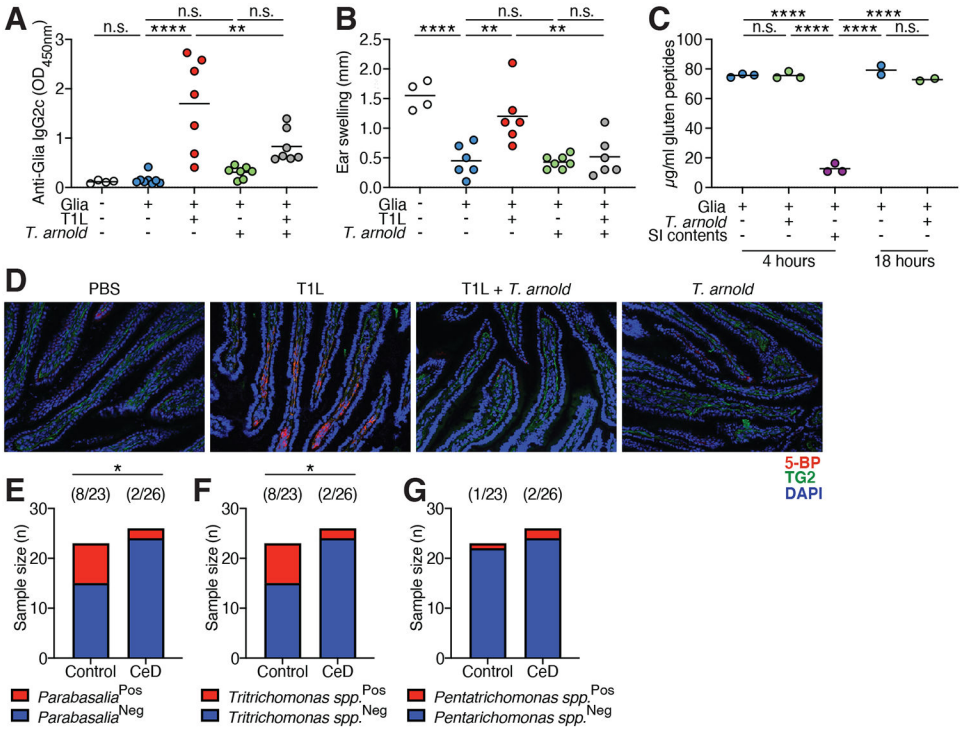

Figure 6. *Parabasalia* protect against LOT to gluten and are underrepresented in CeD patients compared to healthy controls.

(A-B) DTH assay; see schematic in Figure S6A. **(A)** Serum levels of Glia-specific IgG2c antibodies. **(B)** Degree of ear swelling. Data represent two independent experiments (n=4-7 mice/group). **(C)** Amount of remaining Glia measured by G12 antibody, detecting the immunogenic QPQLPY sequence within the 33-mer after *in vitro* Glia- *T. arnold* or small intestinal (SI) content co-incubation at indicated time points (n=2-3 biological replicates/group). **(D)** DQ8tg mice were inoculated perorally with *T. arnold* or PBS for 12 days followed by peroral inoculation with T1L or PBS for 18 hours. TG2 enzymatic activity assessed in the jejunum by 5BP cross-linking is shown in red (nuclei (blue), TG2 protein (green)). Representative images are shown. Scale bars, 50 µm. **(E-G)** Human stool DNA from healthy volunteers and active CeD patients subjected to ITS PCR-DNA sequence analysis. Frequency of **(E)** *Parabasalia* **(F)** *Tritrichomonas* spp. and **(G)** *Pentatrichomonas* spp. detected in healthy and active CeD patients (detected (Pos), not detected (Neg)). Two-sided Fisher's exact test. **(A-C)** Center is mean, one-way ANOVA, Sidak's post hoc test. *$P < 0.05$, **$P < 0.01$, ***$P < 0.001$, ****$P < 0.0001$, n.s. not significant.

KEY RESOURCES TABLE

REAGENT or RESOURCE	SOURCE	IDENTIFIER
Antibodies		
anti-mouse CD45.1 monoclonal antibody (Rat, Clone A20), Brilliant Violet 480 conjugated	BD Biosciences	Cat# 746666; RRID:AB_2743938
anti-mouse CD4 monoclonal antibody (Rat, Clone GK1.5), Brilliant Violet 650 conjugated	BD Biosciences	Cat# 563232; RRID:AB_2738083
anti-mouse CD8a monoclonal antibody (Rat, Clone 53-6.7), Brilliant Violet 570 conjugated	BioLegend	Cat# 100740; RRID:AB_2563055
anti-mouse IFN-gamma monoclonal antibody (Rat, Clone XMG1.2), Brilliant Violet 605 conjugated	BioLegend	Cat# 505839; RRID:AB_2561438
anti-mouse CD45 monoclonal antibody (Rat, Clone 30-F11), APC-R700 conjugated	BD Biosciences	Cat# 565478; RRID:AB_2739257
anti-mouse I-A/I-E monoclonal antibody (Rat, Clone M5/114.15.2), APC/Fire conjugated	BioLegend	Cat# 107652; RRID:AB_2616729
anti-mouse CD45 monoclonal antibody (Rat, 30-F11), Brilliant Violet 480 conjugated	BD Biosciences	Cat# 566095; RRID:AB_2739499
anti-mouse CD4 monoclonal antibody (Rat, GK1.5), BUV395 conjugated	BD Biosciences	Cat# 563790; RRID:AB_2738426
anti-Mouse FOXP3 monoclonal antibody (Rat, Clone FJK-16s), FITC conjugated	Thermo Fisher Scientific	Cat# 11-5773-82; RRID:AB_465243
anti-mouse Tbet monoclonal antibody (Rat, Clone 4B10), APC conjugated	BioLegend	Cat# 17-5825-82; RRID:AB_2744712
anti-mouse Gata3 monoclonal antibody (Rat, TWAJ), PerCP-eFluor 710 conjugated	Thermo Fisher Scientific	Cat# 46-9966-42; RRID:AB_10804487
anti-mouse ROR-gamma(t) monoclonal antibody (Rat, Clone AFKJS-9), PE conjugated	Thermo Fisher Scientific	Cat# 12-6988-82; RRID:AB_1834470
anti-mouse CD44 monoclonal antibody (Rat, Clone IM7), APC conjugated	BD Biosciences	Cat# 103012; RRID:AB_312963
anti-mouse CD62L monoclonal antibody (Rat, Clone MEL-14), PE conjugated	Thermo Fisher Scientific	Cat# 12-0621-81; RRID:AB_465720
anti-mouse CD11b monoclonal antibody (Rat, Clone M1/70), PE-Cyanine7 conjugated	Thermo Fisher Scientific	Cat# 25-0112-82; RRID:AB_469588
anti-mouse CD3 monoclonal antibody (Rat, Clone 17A2), Brilliant Violet 605 conjugated	BD Biosciences	Cat# 564009; RRID:AB_2732063
anti-mouse CD11b monoclonal antibody (Rat, Clone M1/70), APC-eFluor 780 conjugated	Thermo Fisher Scientific	Cat# 47-0112-82; RRID:AB_1603193
anti-mouse CD19 monoclonal antibody (Rat, Clone 1D3), Brilliant Violet 605 conjugated	BD Biosciences	Cat# 563148; RRID:AB_2732057
anti-mouse Ter119 monoclonal antibody (Rat, Clone TER-119), Brilliant Violet 605 conjugated	BD Biosciences	Cat# 116239; RRID:AB_2562447
anti-mouse IL-12p40 monoclonal antibody (Rat, Clone C17.8), PE conjugated	Thermo Fisher Scientific	Cat# 12-7123-82; RRID:AB_466185
anti-mouse TCR β monoclonal antibody (armenian hamster, Clone H57-597), Alexa Fluor 700 conjugated	BD Biosciences	Cat# 560705; RRID:AB_1727573
anti-mouse CD45.1 monoclonal antibody (Rat, Clone A20), APC-R 700 conjugated	Fisher BD	Cat# 565814; RRID:AB_2744397
anti-mouse CD86 monoclonal antibody (Rat, Clone GL-1), Alexa Fluor 647 conjugated	BioLegend	Cat# 105020; RRID:AB_493464

REAGENT or RESOURCE	SOURCE	IDENTIFIER
anti-mouse CD11c monoclonal antibody (Armenian hamster, Clone N418), Brilliant Violet 421 conjugated	BD Biosciences	Cat# 565452; RRID:AB_2744278
anti-mouse CD103 monoclonal antibody (Rat, Clone M290), Brilliant Violet 786 conjugated	BD Biosciences	Cat# 564322; RRID:AB_2738744
anti-mouse F4/80 monoclonal antibody (Rat, Clone BM8), PE-Cyanine5 conjugated	Thermo Fisher Scientific	Cat# 15-4801-82; RRID:AB_468797
anti-mouse I-A/I-E monoclonal antibody (Rat, Clone M5/114.15.2), FITC conjugated	Thermo Fisher Scientific	Cat# 11-5321-82; RRID:AB_465232
anti-DCAMKL1 antibody (ab 31704)	Abcam	Cat# ab31704
Goat anti-rabbit IgG (H+L) antibody, Alexa Fluor Plus 647conjugated	Thermo Fisher Scientific	Cat# A32733; RRID:AB_2633282
Anti-mouse CD326/Ep-CAM, Alexa-Fluor 488 conjugated	BioLegend	Cat# 118210; RRID:AB_1134099
Rabbit polyclonal anti-TG2 antibody	Pacific Immunology	Custom produced
Donkey anti-rabbit IgG (H+L) antibody, Alexa Fluor Plus 488 conjugated	Invitrogen	Cat# A3279; RRID:AB_2762833
Alexa Fluor 594 -Streptavidin conjugated	Invitrogen	Cat# S32356
Goat anti-mouse IgG2c-HRP	SouthernBiotech	Cat# 1078-05; RRID: AB_2794462
anti-mouse I-A/I-E monoclonal antibody (Rat, Clone M5/114.15.2), Brilliant Violet 421 conjugated	BioLegend	Cat# 107632; RRID:AB_2650896
anti-mouse CD45 monoclonal antibody (Rat, 30-F11), BUV395 conjugated	BD Biosciences	Cat# 564279; RRID:AB_2651134
anti-mouse CD11c monoclonal antibody (Armenian hamster, Clone HL3), FITC conjugated	BD Biosciences	Cat# 557400; RRID:AB_396683
anti-mouse CD11b monoclonal antibody (Rat, Clone M1/70), Brilliant Violet 605 conjugated	BioLegend	Cat# 101257; RRID:AB_2565431
anti-mouse CD103 monoclonal antibody (Rat, Clone M290), APC conjugated	BD Biosciences	Cat# 562772; RRID:AB_2737784
anti-mouse CD8a monoclonal antibody (Rat, Clone 53-6.7), BUV737 conjugated	BD Biosciences	Cat# 612759; RRID:AB_2870090
anti-mouse IFN-gamma monoclonal antibody (Rat, Clone XMG1.2), PE-Cyanine7 conjugated	Tonbo Biosciences	Cat# 60-7311; RRID:AB_2621871
anti-mouse CD45.2 monoclonal antibody (Mouse, 104), BUV615 conjugated	BD Biosciences	Cat# 751642; RRID:AB_2875635
anti-mouse KLRG1 monoclonal antibody (Syrian hamster, 2F1), Brilliant Violet 786 conjugated	BD Biosciences	Cat# 565477; RRID:AB_2739256
anti-mouse NK1.1 monoclonal antibody (Mouse, PK136), BUV805 conjugated	BD Biosciences	Cat# 741926; RRID:AB_2871239
Biological Samples		
Patient stool samples (HiREB #12599-T for CeD patients; HiREB #2820 for controls)	Provided by E Verdú, P. Bercik, and H. Galipeau	N/A
Chemicals, Peptides, and Recombinant Proteins		
Zombie NIR™ Fixable Viability Kit	BioLegend	Cat# 423106
LIVE/DEAD™ Fixable Aqua Dead Cell Stain Kit	Invitrogen	Cat# L34957
Super Bright Complete Staining Buffer	eBioscience	Cat# SB-4401-75
Proteinase K Solution	Invitrogen	Cat# 25530049
iTaq™ Universal SYBR® Green Supermix	Bio-Rad	Cat# 1725125
GolgiStop	BD Biosciences	Cat# 554724

REAGENT or RESOURCE	SOURCE	IDENTIFIER
Phorbol 12-myristate 13-acetate (PMA)	Sigma-Aldrich	Cat# P1585
Ionomycin calcium salt	Sigma-Aldrich	Cat# I0634
Golgi Plug	Fisher Scientific	Cat# BDB555029
Percoll	Thermo Fisher Scientific	Cat# 45-001-747
RPMI 1640	Thermo Fisher Scientific	Cat# MT10040CV
Mouse Erythrolysin Lysing Kit	R & D Systems	Cat# WL2000
Penicillin-Streptomycin-Glutamine	Gibco™	Cat# 10-378-016
Collagenase VIII	Sigma-Aldrich	Cat# 10103586001
CellTrace Violet Proliferation Kit	Thermo Fisher Scientific	Cat# C34557
Ovalbumin diet	ENVIGO	Cat# TD.130362
Ovalbumin & Gluten-free control diet	ENVIGO	Cat# TD. 130360
7.7% Wheat Gluten diet	ENVIGO	Cat# TD. 220621
Gluten-free diet	ENVIGO	Cat# AIN76A
Diet with 15 kcal% Fat with 100 g Cellulose	Research Diets	Cat# D17030102
OVA grade V	Sigma-Aldrich	Cat# A5503-25G
OVA peptide (OVA323-339)	Invitrogen	Cat# vac-isq
Recombinant Mouse TGF-beta1	BioLegend	Cat# 240-B-002
Gliadin	Sigma-Aldrich	Cat# 9007-90-3
Complete Freund's Adjuvant	Sigma-Aldrich	Cat# F5881-6X10ML
Succinate	Sigma-Aldrich	Cat# S3674-1KG
EDTA, 0.5M, pH 8.0	Fisher Scientific	Cat# 15-575-020
Tissue-Plus O.C.T. Compound	Fisher Scientific	Cat# 23-730-571
Paraformaldehyde	Fisher Scientific	Cat# AAJ19943K2
4',6-diamidino-2-phenylindole (DAPI)	Thermo Fisher Scientific	Cat# D1306
5-(biotinamido)-pentylamine (5-BP)	Provided by B. Jabri	N/A
Alexa Fluor 647 NHS Ester	Thermo Fisher Scientific	Cat# A20006
Vancomycin	Sigma-Aldrich	Cat# V2002
Gentamycin	Sigma-Aldrich	Cat# G1914
Penicillin	Thermo Fisher Scientific	Cat# SV30010
Streptomycin	Sigma-Aldrich	Cat# S9137-100G
Amphotericin B	Sigma-Aldrich	Cat# 1397-89-3
Media. Lactobacilli MRS Broth	Fisher Scientific	Cat# DF0881-17-5
Recombinant Mouse IL-25	R&D Systems	Cat# 7909-IL-010/CF
Critical Commercial Assays		
FoxP3 Transcription Factor Staining Kit	eBioscience	Cat# 00-5523-00
Cytofix/Cytoperm™ Fixation/Permeabilization Kit	BD Biosciences	Cat# 554714
CD11c Positive Selection Kit II	STEMCELL Technologies	Cat# 18781
TMB Substrate Kit	Bio-Rad	Cat# 34021
iScript™ cDNA Synthesis Kit	Bio-Rad	Cat# #1708891BUN

REAGENT or RESOURCE	SOURCE	IDENTIFIER
RNeasy Plus Mini Kit	Qiagen	Cat# 74136
QIAamp Fast DNA Stool Mini Kit	Qiagen	Cat# 51604
Periodic Acid-Schiff (PAS) Kit	Sigma	Cat# 395B-1KT
V-Plex Mouse IFN-γ Kit	Meso Scale Diagnostics	Cat# K152QOD-1
GlutenTox Competitive ELISA G12	Fisher Scientific	Cat# NC1984116
Experimental Models: Organisms/Strains		
Tritrichomonas arnold	This paper	N/A
Type 1 Lang (T1L)	Provided by T. Dermody	N/A
Murine norovirus strain CW3	Provided by T. Nice	N/A
C57BL/6J	Jackson Laboratory	Cat# 000664
Mouse: $RAG^{-/-}$ $OT\text{-}II^{+/-}$ $CD45.1^{+/+}$	Provided by B. Jabri	N/A
Mouse: HLA-DQ8 transgenic (DQ8tg)	Provided by B. Jabri	N/A
Mouse: IL-18 deficient ($B6.129P2\text{-}Il18^{tm1Aki}/J$)	Jackson Laboratory	Cat# 004131
Oligonucleotides		
Ifnb forward: CCATCCAAGAGATGCTCCAG; *Ifnb* reverse: GTGGAGAGCAGTTGAGGACA	Meisel et al., 2018	N/A
Gapdh forward: AGGTCGGTGTGAACGGATTTG; Gapdh reverse: TGTAGACCATGTAGTTGAGGTCA	Meisel et al., 2018	N/A
28S: TCCTCCGCTTAATGAGATGC; *18S*: AATACGTCCCCTGCCCTTTGT	Chudnovskiy et al., 2016	N/A
28S CTTCAGTTCAGCGGGTCTTC; 18S AACCTGCCGTTGGATCAGT	Chudnovskiy et al., 2016	N/A
28S: GCTTTTGCAAGCTAGGTCCC; *18S*: TTTCTGATGGGGCGTACCAC	Howitt et al., 2016	N/A
IL-27 forward: CTCTGCTTCCTCGCTACCAC *IL-27* reverse: GGGGCAGCTTCTTTTCTTCT	Bouziat et al., 2017	N/A
Murine norovirus forward: ATGGTRGTCCCACGCCAC *Murine norovirus* reverse: TGCGCCATCACTCATCC	Bouziat et al., 2017	N/A
Software and Algorithms		
GraphPad Prism 9	GraphPad Software	N/A
FlowJo 10.7.1	Tree Star	https://www.flowjo.com/solutions/flowjo/downloads
BioRender	BioRender Company	N/A
Nikon NIS Elements Imaging Software	Nikon Instruments	N/A
Adobe Illustrator	Adobe	N/A
CFX Maestro	Bio-Rad	N/A